BACHELOR' S THESIS / BIOMEDICAL ENGINEERING 2024

Multi-scale model for simulating thrombus formation and anticoagulant treatment

Marina Ribera Pascual

Universitat Pompeu Fabra Barcelona

Multi-scale model for simulating thrombus formation and anticoagulant treatment

Marina Ribera Pascual

Bachelor's thesis UPF 2023/2024

Thesis supervisor(s):

Andy L. Olivares, (Physense research group)

Maria Segarra, (Physense research group)

Acknowledgments

I would like to express my sincere gratitude to my thesis supervisors, Andy L. Olivares and Maria Segarra, for their guidance, support and dedication throughout this project. Their expertise has helped me to shape my research and overcome different challenges.

I would like to thank all the members of the PhySense group who participated in the monitoring and development of this project. In particular, I would like to thank Oscar Camara for giving me the opportunity to develop this work and for his guidance throughout this process.

Finally, I would like to thank my family and friends for their support and encouragement that has motivated me throughout my academic journey.

Summary/Abstract

Thrombosis is the localised clotting of blood and has a significant impact on medicine. Thrombi are formed by the activation of a series of events in the coagulation cascade. One way to prevent thrombus formation is by administering anticoagulants, which are drugs that target specific proteins in this cascade. In this work, a coagulation cascade model was developed. It provides a valuable tool for understanding the complex dynamics of thrombus formation and the role of the coagulation factors. Specifically, this model describes the temporal behaviour of several key components, including the tissue factor/factor VII complex, factor XI, factor IX, factor X, prothrombin, thrombin, factor VIII, factor V, protein C, peptide P, inactive and active fibrinogen, fibrin matrix and three intermediate complexes. The increase in viscosity that occurs as the thrombus develops is also described. The influence of tissue factor, factor XI and prothrombin on thrombus formation was also analysed through a sensitivity analysis. Prothrombin was found to have a major influence, as it is the precursor of thrombin, a crucial factor in the coagulation cascade. The coagulation cascade model was coupled to a fluid simulation of an idealised aneurysm, providing a comprehensive view of the spatial-temporal distribution of the coagulation factors based on the integration of residence time. The mapping of coagulation factors allows for a more realistic representation of physiological conditions. Inside the aneurysm, higher concentrations of coagulation factors were observed, as well as the presence of vortices, suggesting thrombus formation inside the aneurysm. In addition, the effect of the anticoagulant warfarin was incorporated into the coagulation cascade model. While warfarin successfully lowered the concentrations of the coagulation factors and delayed their activation, it was insufficient to prevent thrombus formation, as the same concentration was achieved as without anticoagulant.

Keywords

Coagulation cascade modelling, blood coagulation, thrombus formation, residence time, thrombin peak, warfarin monitoring.

Preface

The study of thrombus formation and the coagulation cascade is a crucial area of medical research to improve the understanding and treatment of different cardiovascular diseases. This thesis presents a comprehensive model describing the temporal behaviour of several key components in the coagulation process. Thanks to residence time integration from fluid dynamics simulation concentration of coagulation factors and viscosity is mapped in a 2D idealised aneurysm. Besides, the effect of warfarin, one of the most common administered anticoagulant therapies, was modelled.

The motivation of this work arises from better understand the complex mechanisms underlying blood clot formation and to identify appropriate anticoagulation approaches for each patient. In particular, this research is driven by the need to improve the management of postoperative anticoagulant strategies following left atrial appendage occlusion device implantation. After such interventions, patients must take anticoagulants for a period of time to prevent thrombus formation and foster device endothelization, but there is any standardised protocol for anticoagulant administration.

This thesis provides a coagulation cascade model that can serve as a basis for future research, with the potential to improve the ability to predict and prevent thrombus formation in patients with cardiovascular disease.

Index

List of figures

List of tables

1. INTRODUCTION

1.1 Thrombus formation

When an injury occurs in the wall of a vessel that causes blood to escape from the circulation, a series of events are triggered to try to seal the breach. These events are rapidly activated both in the vessel wall and in the blood. This process is known as haemostasis and aims to preserve the integrity of a closed, high-pressure circulatory system after vascular damage [1].

The endothelium contains three thromboregulators (nitric oxide, prostacyclin and the ectonucleotidase CD394), which prevent thrombus formation. When a pathological phenomenon occurs, homeostasis is altered (i.e., the internal environment of the body is no longer in equilibrium), and excessive quantities of thrombin form, leading to thrombus initiation [1].

Thrombus formation is the result of the coagulation cascade activation and presents a heterogeneous composition; it primarily consists of fibrin and other components that includes platelets and red blood cells (Figure 1) [2]. Its architecture and proportion of each component is influenced by shear, flow, turbulence and the number of platelets in the circulation [1]. This fact makes it possible to classify thrombi into red and white thrombi. The generation of white thrombi, also known as arterial thrombi, is enhanced under conditions of high shear and altered blood flow, leading to amplified platelet recruitment. In contrast, the generation of red thrombi, also known as venous thrombi, is enhanced under conditions of slow blood flow, leading to increased production of fibrin which traps a significant number of erythrocytes [3].

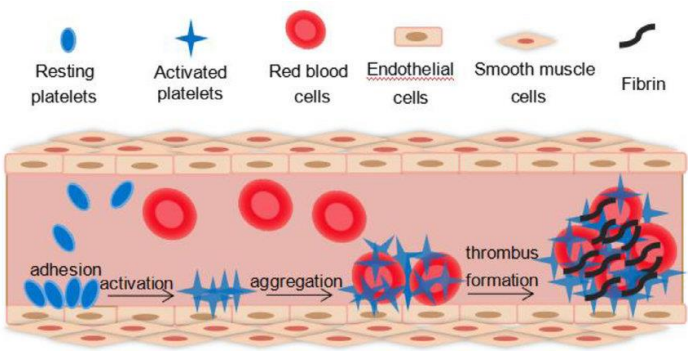

Figure 1. Thrombus formation process in a blood vessel [4].

1.1.1 Virchow's triad

More than a century ago, Rudolf Virchow described the three main factors involved in thrombus formation, known as Virchow's triad. The three factors involved are the following: blood stasis, hypercoagulability, and endothelial dysfunction [5].

Blood flow regulates vascular reactivity as well as platelet adhesion and aggregation. In addition, depending on the stress on the vessel wall, prothrombotic and proinflammatory endothelial mediators are secreted. Thus, if blood flow is interrupted, erythrocytes, leukocytes and platelets approach the vessel wall, causing their adhesion and activation [6].

A healthy endothelium plays a crucial role in maintaining a haemostatic environment. However, pathological processes can cause cleavage or detachment of certain molecules, contributing to an impaired or dysfunctional endothelium. The resulting increase in plasma levels of these molecules may shift haemostasis toward pro-coagulation [6].

Hypercoagulability mainly affects the activation of the coagulation cascade. Specifically, it is related to increased platelet reactivity or impaired fibrinolysis [5].

When the coagulation system is altered, a pro-thrombotic condition is promoted through the mechanisms described in Virchow's triad, increasing the risk of thrombus formation.

1.1.2 Coagulation cascade

The coagulation cascade is classically described as consisting of three pathways: extrinsic, intrinsic and common pathways (see Figure 2). The first two converge at the same point, activating factor X, which initiates the common pathway, ultimately leading to clot stabilization [3]. Furthermore, this coagulation cascade can be divided into three stages: initiation, amplification and propagation, as can be seen in Figure 3 [7].

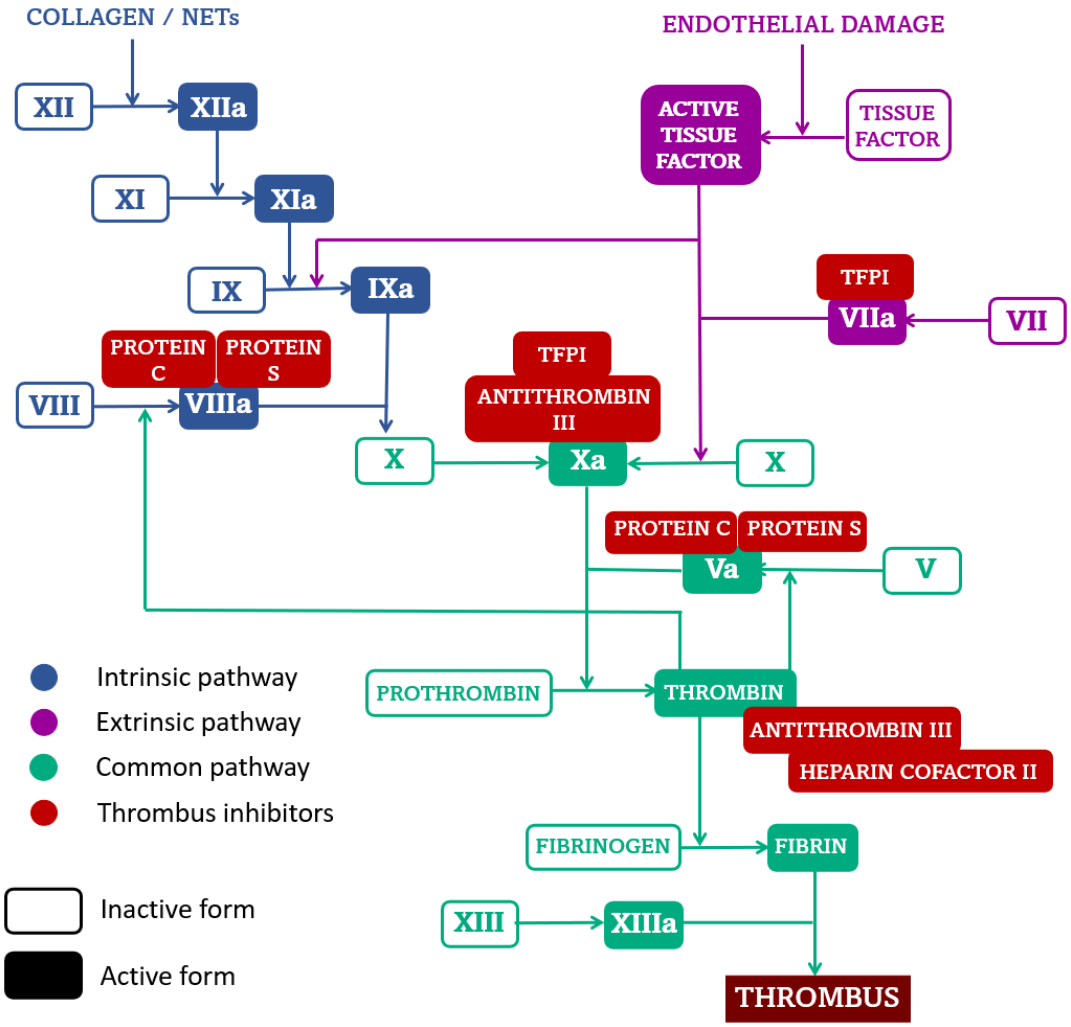

Figure 2. Coagulation cascade.

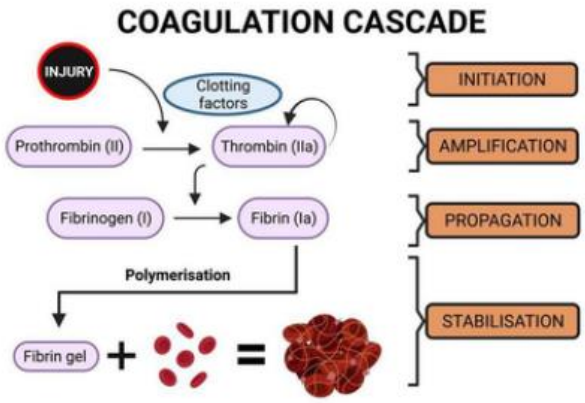

Figure 3. Simplified coagulation cascade for thrombus formation [8].

Thrombus formation can be initiated after an external damage, which would trigger the activation of the coagulation cascade. The wall injury causes collagen and tissue factor to be exposed [9].

The extrinsic pathway is initiated by the exposed tissue factor, which, in its active form, activates factor VII. The combination of both factors forms a complex that activates factor X [3, 10]. Both this complex and factor X are inhibited by the plasma protease inhibitor (TFPI) [3].

The intrinsic pathway is related to the collagen exposed, which leads the activation of factor XII and causes the circulating platelets to be attracted and activated [1]. Additionally, the intrinsic pathway can also be activated by the release of neutrophil extracellular traps (NETs), contributing to its activation in pathological conditions [3]. The activation of factor XII leads to the activation of factor XI, which in turn leads to activation of factor IX [10]. The latest factor is also activated by the complex formed by tissue factor and factor VII [7]. Activated factors IX and VIII, lead to the activation of factor X. Factor VIII and factor V are both inhibited by proteins S and C. The von Willebrand factor also plays a role in this pathway, acting to stabilize factor VIII in addition to promoting platelet adhesion and aggregation [3].

Both the extrinsic and intrinsic pathways constitute the initiation stage of coagulation. Also in this stage, activated factor X results in the activation of small amounts of thrombin before the TFPI is activated [7].

The amplification stage involves the activation of the first part of the common pathway, which begins with the activation of factor X through both the extrinsic and intrinsic pathways. As mentioned before, factor X is inhibited by TFPI, but it is also inhibited by antithrombin III. Active factor X converts prothrombin into thrombin, also referred to as factor II. Thrombin is a crucial enzyme in the coagulation cascade and is inhibited by antithrombin III and heparin cofactor II. It acts as a feedback activator, triggering the activation of platelets, factor V and factor VIII [3]. Activated platelets release some agonists that activate other platelets producing an amplification of the signal for thrombus formation. They are also involved in the release of certain enzymes that contribute to tissue factor activation and fibrin formation [1]. Moreover, platelets provide the surface on which activated factors assemble, forming a functional coagulation complex [7].

Coagulation only proceeds to the propagation stage if there are enough clotting factors and activated platelets [7]. At this stage, significant thrombin production occurs on the

surface of platelets. This triggers the conversion of fibrinogen into fibrin monomers. Subsequently, the fibrin clot consolidates as fibrin strands form covalent bonds, a process catalysed by factor XIII [3]. Finally, an interconnected fibrin mesh forms, trapping platelets and blood cells. This final mesh produces a haemostatic plug, effectively sealing the area of endothelial injury and promoting healing [8]. During this process, not all recruited platelets are activated; others remain associated with the thrombus without activation and may detach [1].

1.2 Thrombus formation treatments

In order to prevent the formation of thrombus, different approaches have been developed and implemented. There are two principal pharmacological ways to treat thrombus formation. Drugs that target proteins of the coagulation cascade and drugs that target platelets are administered. Although the antithrombotic drugs available are effective in reducing thrombus formation in patients with cardiovascular disease, their use is limited by the risk of bleeding [11].

1.2.1 Anticoagulants

Oral anticoagulants are recommended for most patients with atrial fibrillation, as they are capable of preventing the majority of ischemic strokes in these patients, and for patients to prevent venous thromboembolism [11, 12]. However, identifying the correct dose is a crucial point in the clinical practice and individualisation of oral anticoagulant therapy [13].

The standard treatment for the prevention of thrombus formation is vitamin K antagonists (VKAs) [12, 14]. This type of anticoagulant acts on vitamin K-dependent coagulation factors, such as prothrombin, factors VII, IX, X, protein C and protein S [14]. Vitamin K antagonists are prescribed for long-term anticoagulant treatment [11]. One of the most common is warfarin [15]. This type of anticoagulant, by inhibiting the reduction reaction in the vitamin K cycle, prolongs the prothrombin time (PT), which is one of the most common measurements of coagulation activity [14]. This measurement involves assessing the time it takes for plasma to clot after adding thromboplastin, which is a mixture of tissue factor, calcium and phospholipid to a patient’s plasma sample [16].

However, the use of VKAs is associated with a risk of severe, fatal, intracranial and gastrointestinal haemorrhage, a narrow therapeutic profile and numerous diet-drug interactions [15, 17]. For this reason, alternatives have been developed that offer an improved balance between efficiency and safety, fewer interactions with food and drugs and allow a fixed dose regimen without the need for routine coagulation monitoring [12, 13]. Specifically, there are four direct oral anticoagulants (DOACs) that inhibit thrombin (dabigatran) and factor Xa (rivaroxaban, apixaban and edoxaban). DOACs have surpassed VKAs by decreasing intracranial haemorrhage, which is why they have begun to replace them [12]. However, there is currently less guidance and research available on these alternatives compared to VKAs [13].

Heparins are a type of anticoagulant that act by binding to antithrombin, thereby increasing its ability to inhibit factor X and thrombin. It is currently prescribed in cases of cardiovascular surgery and for the prevention of venous thromboembolism. However, these anticoagulants can lead to the generation of specific antibodies that can activate platelets, thereby generating thrombin and causing thrombosis [11].

1.2.2 Antiplatelets

Antiplatelet drugs can both reduce thrombus growth for acute thrombotic events and can be used prophylactically to reduce the incidence of arterial thrombosis. They mainly target molecules that are related to platelet activation and aggregation [11]. The most widely used antiplatelet agents globally include aspirin, clopidogrel, and dipyridamole. However, there are patients who experience ischaemic events while taking antiplatelet agents, develop adverse effects due to use, or develop allergic reactions. Importantly, antiplatelet agents are associated with an increased risk of bleeding when administered for long-term prevention although they have a lower recurrence of stroke in the short term [18].

1.3 Multi-scale models of thrombus formation

In clinical practice it is essential to identify the appropriate dose of anticoagulant to prevent thrombus formation. To determine the dose and prevent thrombus formation, it is essential to know the mechanisms that trigger their formation. For this purpose, computational fluid dynamics (CFD) modelling is a very useful tool, allowing to observe regions of turbulent flow that may be associated with thrombus development. However, CFD simulations do not account for the needed biological details to consider hypercoagulability. Therefore, to capture the complexity of the coagulation cascade, computational systems biology techniques represent a promising tool. These techniques involve systems of equations, specifically ordinary differential equations (ODEs), that model the reactions within the system.

For several decades, systems of ordinary differential equations have been developed with the aim of obtaining a model of the coagulation cascade, or at least part of it [7, 19, 20]. Usually, the coagulation cascade models are quantitative and not Boolean or semiquantitative as the reactions involved are relatively well characterized experimentally. This makes that the definition of equations are easier than in other context in which the reactions are not exhaustively known (i.e., such when modelling the regulatory pathways of cells [21]). However, the scientific community have not reached a consensus establishing a defined systems of equations that maps efficiently the reactions involved in the coagulation process. In a study by Xu *et al*., [7] six differential equations were developed, most of them following the first order mass action law to evaluate thrombin generation. Additionally, the study assessed the stimulus that triggers the coagulation cascade and examined how the platelet ratio affects thrombin concentration. The equations mentioned considered factors from the extrinsic, intrinsic and common pathways. Specifically, for the extrinsic pathway it considered a complex formed by both tissue factor and factor VII. For the intrinsic pathway it considered factors IX and VIII. For the common pathway, it considered factors X, V and thrombin. In a study by Zarnisina *et al*., [19] a mathematical model focusing on the intrinsic pathway was developed, incorporating eight differential equations. These equations describe the spatiotemporal dynamics of factors within both the intrinsic pathway, including factors XI, IX and VIII, and the common pathway, involving factors X, V, prothrombin, thrombin and fibrin, as well as the coagulation inhibitor protein C. The equations describing factor IX, X, fibrin, protein C and peptide P follow the first order mass action law, while the equations describing factor VIII and V follow both first and second order mass action laws. As for the equations for both prothrombin and thrombin, they follow the Michaelis-Menten kinetics to a greater extent, assuming irreversibility in this step. Finally, in a study by Pearce *et al.*, [20] 7 differential equations were developed to model the polymerisation

of the fibrin matrix. For this, only the final part of the common pathway was considered, in particular from thrombin generation. In this case all the equations use the law of mass action. For the model, the dynamic interactions between thrombin, fibrinogen, fibrin and three intermediate complexes were contemplated.

Some published coagulation cascade models include the effect of some type of anticoagulant therapy [14, 22]. In a study by Wajima *et al*., [14] a series of differential equations were developed to model 51 components of the coagulation cascade. These equations considered factors from the three pathways of the coagulation cascade, i.e., the extrinsic, intrinsic and common pathways. In addition, the model also included the vitamin K cycle and its action on the coagulation reactions. The incorporation of the vitamin K was key to introduce the effects of the vitamin K dependent anticoagulants. In fact, the model was used to simulate anticoagulant therapy with warfarin and heparin. In a study by Burghaus *et al*., [22] a model that considered both the intrinsic and extrinsic pathways of the coagulation cascade was developed. Additionally, factors from the common pathway such as thrombin and fibrin were also considered, with the formation of the latter being regarded as a cleavage product of fibrinogen. Furthermore, some of the proteins that trigger the inhibition of the coagulation cascade were also taken into account. This study evaluated the efficacy and safety of different doses of rivaroxaban and compared the mechanisms of action with warfarin.

CFD have been developed to analyse the blood flow associated with thrombus formation, without taking into account the coagulation cascade [23, 24, 25]. In the study by Hatoum *et al*., [23] the geometry of six patients after transcatheter aortic valve replacement was used. Using vorticity flux metrics from CFD models was shown to predict the likelihood of leaflet thrombosis with promising sensitivity and specificity. In the study by Mill *et al*., [24] flow simulations of specific patients presenting left atrial appendage occlusion were carried out to identify key blood flow characteristics that lead to device related thrombus. In the study by Gasoarotti *et al*., [25] the hemodynamic effects of different left atrial appendage occlusion devices were studied. Specific models of patients with three different types of implanted devices were used. CFD was analysed before and after device implantation and pressure, velocity and main hemodynamic indices were evaluated to assess the risk of thrombus formation.

Finally, it is worth noting that CFD models have also been carried out coupled to coagulation cascade models [26, 27, 28]. The two-dimensional spatial-temporal distribution of species of the intrinsic and common pathway of the coagulation cascade has been analysed. This is the case of the Guerrero-Hurtado *et al*., [26] study, in which they propose a multi-fidelity strategy to increase the efficiency of coagulation cascade simulations in a non 0D context. To do so, they used ODEs that represent the evolution of species concentrations as a function of blood residence time. They expanded the solution of the ODEs around the zero-diffusivity limit in Taylor series to obtain practical approximations of how chemical species concentrations are distributed in space and time, using statistical moments of residence time as a basis. The developed model was applied to an idealised aneurysm geometry. It should be noted that they do not consider the extrinsic pathway. In a study by Qureshi *et al*., [27] simulations were performed on two patient-specific models of the left atrial to evaluate the three factors of Virchow's triad in both sinus rhythm and atrial fibrillation. To do so, blood stasis and endothelial cell activation potential (which is a metric of endothelial damage) of both left atrial models were quantified. Additionally, only the final part of the coagulation cascade was considered, specifically thrombin, fibrinogen and fibrin, to evaluate hypercoagulability,

solving the reaction-diffusion-convection equations for these three factors. This study allowed for the evaluation of Virchow's triad factors to quantify the risk of stroke in two specific patients. Finally, in another study by Qureshi *et al*., [28] the geometry of the left atrium from a single patient was used, testing both sinus rhythm and atrial fibrillation. In the study, all aspects of Virchow's triad were also integrated, including blood stasis, endothelial damage via the endothelial cell activation potential, and hypercoagulability using reaction-diffusion-convection equations only for thrombin, fibrinogen and fibrin. In this case, a new method for quantifying thrombus growth was proposed.

No work can be found in the literature with complete models of the coagulation cascade coupled to fluid simulations that allow to observe the behaviour of anticoagulants. Models of the coagulation cascade are often incomplete, lacking the extrinsic pathway. In addition, due to the importance of administering the appropriate dose of anticoagulants, it would be useful to obtain a complete model to predict the ideal treatment for each patient. Both the appropriate dose and the time that treatment should be administered, in order to reduce the number of drugs taken by the patient.

1.4 Objectives

The project has two main objectives. Firstly, to develop a computational multi-scale model of thrombus formation coupled with fluid simulations in an idealized geometry. Secondly, to model the influence of anticoagulants when combined with thrombus formation. For this purpose, a multi-scale model is performed, in order to take into account the cascade that produces thrombus formation. To do so, the following specific tasks have been developed:

- Modelling the behaviour of thrombin, fibrinogen and fibrin in 0D by using reaction equations and consider the effect of different anticoagulants.
- Modelling thrombus formation considering the coagulation cascade and coupling it with fluid simulations in two-dimensional geometries and consider the effect of different anticoagulants.
- Analyse which parameters can be personalised for each patient with a sensitivity analysis.

This would improve our understanding of thrombogenesis under flow conditions. Such models would improve the management of the treatment strategies in patients at risk for thrombosis.

2. METHODS

Blood coagulation is regulated by a number of interrelated biological processes, such as protein adsorption, platelet activity, the complement system and coagulation reactions [29]. The transport and reaction of coagulation factors play a crucial role in these processes as they ensure that the necessary factors are administered and activated at the right places and times. Therefore, thrombus formation is a multi-scale event, as it starts with chemical reactions at the molecular level, resulting in thrombus formation at the tissue level [30, 31]. Furthermore, these processes are influenced by cardiac geometry at a larger scale.

2.1 0D model of the coagulation cascade

In order to develop a mathematical model that captures all the critical steps of the coagulation cascade, it was based on the differential equations of different existing models of the coagulation cascade [7, 19, 20]. The resulting model had to consider that the coagulation process evolves over time and that each factor is activated at different points in the process.

The extrinsic pathway of the coagulation cascade model was based on the equations of Xu *et al*. [7]. From this model, only the differential equation that accounts for the formation of tissue factor (TF) and the activated factor VII (VIIa) complex (TF:VIIa) was considered. The following equations assumes that all the TF reacts with VIIa forming a complex:

$$\frac{dTF{:}VIIa}{dt} = k_1\beta - h_1 \cdot TF{:}VII_a \cdot X_a \tag{1}$$

In Equation 1 the first term on the right side summarizes how the complex is formed. It assumes that there is a constant stimulus that promotes the formation of a limited amount of TF and that all TF reacts to form the TF:VIIa complex. The kinetic constant (k_1) determines the reaction rate, while β denotes the strength of the stimulus. The remaining term of the right side describes how TF:VIIa complex is inhibited by the binding of itself and factor X. The constant h_1 represents a dissipation or dissociation coefficient and considers the inhibition due to TFPI. All these constats are listed in Table 1 in S.1.

The intrinsic pathway and the initial part of the common pathway (up to thrombin formation) of the coagulation cascade model were based on the work of Zarnitsina *et al*. [19]. These equations were based on biochemical data on blood coagulation at various stages of the process. Moreover, they were verified by comparing experimentally obtained measurements of the kinetics of thrombin generation at different calcium concentrations [19]. The differential equations considered were for the activated factor XI (XIa), activated factor IX (IXa), activated factor X (Xa), thrombin (IIa), prothrombin (II), activated factor VIII (VIIIa), activated factor V (Va) and activated protein C (PCa). In addition, the peptide P (P) was also considered. In some of the factors, terms proposed by Xu *et al*. [7] concerning the extrinsic pathway were added.

$$\frac{dXIa}{dt} = k_{11} \cdot\ II_a - h_{11} \cdot\ XI_a \tag{2}$$

$$\frac{dIXa}{dt} = k_{3x} \cdot\ TF{:}VII_a + k_9 \cdot\ XI_a - h_9 \cdot\ IX_a \tag{3}$$

$$\frac{dXa}{dt} = k_{2x} \cdot\ TF{:}VII_a + k_{10} \cdot\ IX_a + \overline{k_{10}} \cdot \frac{k_{89} \cdot IX_a \cdot VIII_a}{h_{89} + k_a \cdot PC_a} - h_{10} \cdot\ X_a \tag{4}$$

$$\frac{dIIa}{dt} = k_2 \cdot\ X_a \cdot \frac{II}{II + K_{2m}} + \overline{k_2} \cdot \frac{k_{510} \cdot X_a \cdot V_a}{h_{510} + k_a \cdot PC_a} \cdot \frac{II}{II + \overline{K_{2m}}} - h_2 \cdot\ II_a \tag{5}$$

$$\frac{dII}{dt} = -k_2 \cdot\ X_a \cdot \frac{II}{II + K_{2m}} - \overline{k_2} \cdot \frac{k_{510} \cdot X_a \cdot V_a}{h_{510} + k_a \cdot PC_a} \cdot \frac{II}{II + \overline{K_{2m}}} \tag{6}$$

$$\frac{dVIIIa}{dt} = k_8 \cdot\ II_a - k_a \cdot\ PC_a \cdot \left(VIII_a + \frac{k_{89} \cdot IX_a \cdot VIII_a}{h_{89} + k_a \cdot PC_a}\right) - h_8 \cdot\ VIII_a \tag{7}$$

$$\frac{dVa}{dt} = k_5 \cdot\ II_a - k_a \cdot\ PC_a \cdot \left(V_a + \frac{k_{510} \cdot X_a \cdot V_a}{h_{510} + k_a \cdot PC_a}\right) - h_5 \cdot\ V_a \tag{8}$$

$$\frac{dPCa}{dt} = \frac{k_{apc1} \cdot k_p + k_{apc2} \cdot P}{k_p + P} II_a - h_{apc} \cdot PC_a \quad (9)$$

$$P = \frac{(k_{apc2} \cdot II_a - h_p \cdot k_p) + \sqrt{(k_{apc2} \cdot II_a - h_p \cdot k_p)^2 + 4 \cdot k_{apc1} \cdot k_p \cdot h_p \cdot II_a}}{2h_p} \quad (10)$$

In Equation 2 the first term on the right side summarizes how factor XIa is formed from thrombin. The remaining term of the right side describes how factor XIa is degraded by passive degradation.

In Equation 3, the initial term on the right side accounts for the formation of factor IXa due to the TF:VII complex. The term next to it also refers to the formation of this factor, but due to factor XIa. The last term represents its inhibition, which depends on its concentration and refers to degradation due to antithrombin III.

Equation 4 refers to the factor Xa. The first two terms on the right side refer to its formation, one due to the TF:VIIa complex and the other due to factor IX. The next term describes the interaction of factors IXa and VIIIa that results in the activation of factor X, this interaction being modulated by the presence of activated protein C. The last term represents its inhibition, which depends on its concentration and refers to degradation due to antithrombin III.

Equation 5 refers to thrombin. The initial term on the right side refers to its generation by the action of factor Xa and prothrombin. The next term describes the interaction of factors Xa, Va and prothrombin that leads to thrombin activation, this interaction being modulated by the presence of activated protein C. The last term represents its inhibition, which depends on its concentration and refers to degradation due to antithrombin III. Prothrombin modulates thrombin formation with Michaelis Menten kinetics.

The initial term on the right-hand side of Equation 6 refers to the degradation of prothrombin through the action of factor Xa and prothrombin itself. The next term describes the interaction of factors Xa, Va and prothrombin that results in the degradation of prothrombin, this interaction being modulated by the presence of activated protein C. These reactions are the ones that produce thrombin.

In Equation 7, the first term on the right side summarises how factor VIIIa is formed from thrombin. The next term represents the total inhibition of factor VIIIa due to activated protein C both directly and through its interaction with factor IXa. The last term refers to passive degradation.

In Equation 8, the initial term on the right side describes the formation of factor Va from thrombin. The subsequent term accounts for the overall inhibition of factor Va by activated protein C, both directly and through its interaction with factor Xa. The final term pertains to passive degradation.

In Equation 9, the first term on the right side summarizes how activated protein C is formed by thrombin. It is activated through two pathways: one pathway dependent on a constant and another dependent on peptide P. The relative contribution of these two pathways is modulated by a Michaelis-Menten kinetics based on the concentration of peptide P. The last term refers to its inhibition, which depends on its concentration and refers to inhibitors present in the plasma.

Equation 10 represents an equilibrium between peptide P activation by thrombin via two pathways, and P-clearance regulated by a constant.

The rate constants present in the model were estimated from *in vitro* kinetics in purified systems of isolated factors [19]. All the constants are listed in Table 2 in S.1.

The formation of the fibrin mesh from thrombin in the coagulation cascade model was based on the equations of Pearce *et al*. [20]. These equations describe the dynamic interactions that occur between thrombin, fibrinogen, fibrin and three intermediate complexes. This provides a model of fibrin matrix polymerisation that consists of the stabilisation of the coagulation cascade. The first stage considered by this part of the model involves the activation of inactive fibrinogen into active fibrinogen following Michaelis Menten-type reaction kinetics, depending on thrombin, and producing a single intermediate complex (C_0). As for fibrin matrix formation, the two-reaction system includes two intermediate complexes. One reaction involves the thrombin-mediated formation of fibrin matrix from active fibrinogen, producing an intermediate complex (C_1). The other reaction also involves the formation of fibrin matrix from active fibrinogen but is mediated by the previous intermediate complex (C_1) and produces another intermediate complex (C_2). The model of Pearce *et al*. [20] considers all reactions as reversible and therefore follows Briggs-Haldane kinetics, except fibrinogen activation, which is considered irreversible and therefore follows Michaelis Menten kinetics. To adjust the model for physiologically accurate results, the conversion of the C_2 complex to fibrin and C_1 complex were considered irreversible. The differential equations considered were for the active fibrinogen (Fbna), fibrin matrix (FM), inactive fibrinogen (Fbni), C_0, C_1 and C_2, and are presented in equations 11 to 16, respectively.

$$\frac{dFbna}{dt} = -k_1^+ Fbna \cdot Thb + k_1^- C_1 - k_3^+ Fbna \cdot C_1 + k_3^- C_2 + kC_0 \quad (11)$$

$$\frac{dFM}{dt} = k_2^+ C_1 - k_2^- Thb \cdot FM + k_4^+ C_2 \quad (12)$$

$$\frac{dFbni}{dt} = -k^+ Fbni \cdot Thb + k^- C_0 \quad (13)$$

$$\frac{dC_0}{dt} = k^+ Fbni \cdot Thb - k^- C_0 - kC_0 \quad (14)$$

$$\frac{dC_1}{dt} = k_1^+ Fbna \cdot Thb - k_1^- C_1 - k_2^+ C_1 + k_2^- Thb \cdot FM + k_3^- C_2 - k_3^+ Fbna \cdot C_1 + k_4^+ C_2 \quad (15)$$

$$\frac{dC_2}{dt} = k_3^+ Fbna \cdot C_1 - k_3^- C_2 - k_4^+ C_2 \quad (16)$$

In terms of the parameters used, in the study by Pearce *et al*. [20] a tailored parameter subset selection technique was developed to identify those parameters that were relevant and representative of the data observed in an *in vitro* experiment on fibrin accumulation. The constants used refer to reaction rates and were assumed to be non-negative. All the constants are listed in Table 3 in S.1.

For the model, a duration of 10 minutes was considered. This duration was chosen to ensure that all relevant events of the coagulation cascade are captured. The initial conditions are given in Table 4 in S.1. As for the other factors, it was considered that they were initially not present. The differential equations were solved using the Runge-Kutta method of order 4 in Matlab R2022b [32].

2.1.1 Viscosity change

During the coagulation cascade, it goes from insoluble fibrin monomers that are dispersed in liquid blood to a polymerized fibrin gel that is semi-solid and will end up as the final thrombus [33]. This process of solidification of the thrombus causes an increase in the viscosity of the blood in that area [34].

To replicate the cooperative solidification mechanism of thrombus formation and the consequential alterations in viscosity (μ), the viscosity of the fibrin gel was modelled, drawing a parallelism to the consistency of liquid clay. Subsequently, the Hill equation was employed to scale viscosity across the entire affected region. Equation 17 presents the viscosity equation where K is 0.5, n is 3, and ϕ represents the ratio between fibrin and fibrinogen (Equation 18). μ_{max} denotes the maximum achievable viscosity of the blood, set at 0.056 Pa·s [35], while μ_{blood} refers to the viscosity of blood in regular conditions, which is $3.5 \cdot 10^{-3}$ Pa·s [33].

$$\mu = \frac{\mu_{max}\,\phi^n}{K^n + \phi^n} + \mu_{blood} \tag{17}$$

$$\phi = \frac{Fibrin}{Fibrinogen} \tag{18}$$

2.1.2 Sensitivity analysis

To determine the influence of some parameters of the coagulation cascade, a sensitivity analysis was conducted. For this purpose, the variation in the initial conditions of three factors was evaluated, specifically the TF:VIIa complex, factor XIa, and prothrombin. The first two were chosen because they were the initial factors in both the extrinsic and intrinsic pathways of the model. Prothrombin was selected because it was the precursor to thrombin, which is a crucial factor in the coagulation cascade. A range of physiological concentrations were selected for each of the chosen factors, as detailed in Table 5 in S.2. Subsequently, 27 different parameter combinations were generated according to a factorial design. This involves combining three levels of each factor in all possible combinations, allowing for the evaluation of both the main effects of each factor and their interactions. Simulations were then performed for all possible combinations of the selected factors' initial conditions, resulting in a comprehensive exploration of the parameter space [36]. In all simulations, $8.823 \cdot 10^6$ nM of inactive fibrinogen was added as an initial concentration.

For each simulation, parameters of both thrombin and fibrin were measured. Regarding thrombin, the maximum concentration and the time between the peak concentration and its disappearance were assessed. This is because thrombin plays a significant role in the coagulation cascade by amplifying the signal, activating platelets, and converting fibrinogen into fibrin. As for fibrin, the concentration reached at the end was measured since the fibrin mesh is the final product of the coagulation cascade.

These results were then subjected to an analysis of variance (ANOVA) to identify which factors most affected the parameters analysed. Firstly, for each factor the Total Sum of Squares (TSS) was calculated (Equation 19), allowing the total variance of the factors to be represented.

$$TSS_f = \sum_{s=1}^{27} (p_s - \bar{p})^2 \tag{19}$$

p_s refers to the value of the parameter of each factor, and $\bar{p}$ refers to the mean of the parameters of all the simulations. Next, the partial sum of squares (PSS) was calculated to determine the effect of one parameter on a specific factor (Equation 20).

$$PSS_f^{param} = \sum_{s=1}^{3}(p_s - \bar{p})^2 \quad (20)$$

Finally, a measure of significance was calculated for each factor and parameter (Equation 21).

$$I_f^{param} = \frac{PSS_f}{TSS_f} \cdot 100 \quad (21)$$

This allowed each parameter to be ranked according to the influence of each factor.

2.2 Effect of anticoagulant

In an attempt to assess the effect of anticoagulants on the coagulation cascade, a term was added to the factors that were affected by the anticoagulant. The anticoagulant of choice was warfarin, as it is one of the most widely used anticoagulants to prevent thrombus formation [11]. Since warfarin indirectly acts on prothrombin, factor VII, factor IX, factor X, protein C and protein S, the anticoagulant was applied in the differential equations corresponding to these factors. It was applied in the equations of the TF:VIIa complex factor IXa, factor Xa, prothrombin and active protein C, the rest of the equations remained the same. The modified equations correspond to equations 22 to 26.

$$\frac{dTF{:}VIIa}{dt} = k_1\beta\left(1 - \frac{kw \cdot warfarin}{ke}\right) - h_1 \cdot TF{:}VII_a \cdot X_a \quad (22)$$

$$\frac{dIXa}{dt} = k_{3x} \cdot TF{:}VII_a\left(1 - \frac{kw \cdot warfarin}{ke}\right) + k_9 \cdot XI_a - h_9 \cdot IX_a \quad (23)$$

$$\frac{dXa}{dt} = k_{2x} \cdot TF{:}VII_a\left(1 - \frac{kw \cdot warfarin}{ke}\right) + k_{10} \cdot IX_a - \overline{k_{10}} \cdot \frac{k_{89} \cdot IX_a \cdot VIII_a}{h_{89} + k_a \cdot PC_a} - h_{10} \cdot X_a \quad (24)$$

$$\frac{dII}{dt} = -k_2 \cdot X_a \cdot \frac{II}{II + K_{2m}}\left(1 - \frac{kw \cdot warfarin}{ke}\right) - \overline{k_2} \cdot \frac{k_{510} \cdot X_a \cdot V_a}{h_{510} + k_a \cdot PC_a} \cdot \frac{II}{II + \overline{K_{2m}}} \quad (25)$$

$$\frac{dPCa}{dt} = \frac{k_{apc1} \cdot k_p + k_{apc2} \cdot P}{k_p + P} II_a\left(1 - \frac{kw \cdot warfarin}{ke}\right) - h_{apc} \cdot PC_a \quad (26)$$

The term corresponding to warfarin effect refers to how much the production of coagulation factors is reduced due to warfarin inhibition. This term was applied to the production of each affected factor since the anticoagulant inhibits its production. Except in the case of prothrombin, that warfarin was added to its degradation since what is affected is its conversion to thrombin. This inhibition depends on the warfarin concentration, and a factor kw and ke. The kw is a normalized inhibition ratio. The ke refers to the ratio between clearance and distribution volume of the anticoagulant, i.e., it provides information on how it is eliminated and distributed in the body. kw multiplied by the warfarin concentration represents the effective amount of inhibition. Dividing by ke normalizes the inhibitory effect to the pharmacokinetics of warfarin in the patient. The inhibitory effect is subtracted from one so that as the concentration of warfarin is reduced, the effect on the production of coagulation factors is smaller.

As for the behaviour of warfarin, it was assumed that the peak of maximum concentration in blood occurs at the beginning of the simulation and gradually decreases in concentration (Equation 27). The rate at which warfarin concentration decreases depends on the absorption rate constant (ka_{war}).

$$\frac{dwarfarin}{dt} = -ka_{war} \cdot warfarin \tag{27}$$

From the study of Wajima *et al.*, [14] k_e was considered to have a value of 0.02 hr^{-1} and ka_{war} was considered to have a value of 1.0 hr^{-1}. The k_w factor was defined with a value of $6.32 \cdot 10^{-8}$.

In a study of Kwon *et al*., [37] the mean plasma concentration of warfarin was analysed in 105 patients. So, for the anticoagulant model, this concentration of warfarin, which was 1.3 mg/L, was considered as the initial concentration. In addition, the simulation was considered to last 10 minutes and the initial concentrations were as listed in Table 4 S.1. As for the other factors, it was considered that they were initially not present. The differential equations were solved using the Runge-Kutta method of order 4 in Matlab R2022b [32].

2.3 Coagulation cascade in a 2D aneurysm

In order to evaluate the spatial-temporal distribution of the factors involved in the coagulation cascade as well as the changes in viscosity, the model of the coagulation cascade was extended in an idealised two-dimensional geometry. Specifically, the geometry of an idealised aneurysm from the study of Guerrero-Hurtado *et al.*, [26] was used so that our results can be benchmarked with theirs.

The aneurysm geometry consisted of a tube of diameter H representing the blood vessel and a circular cavity of radius 0.75H representing the aneurysm (Figure 4).

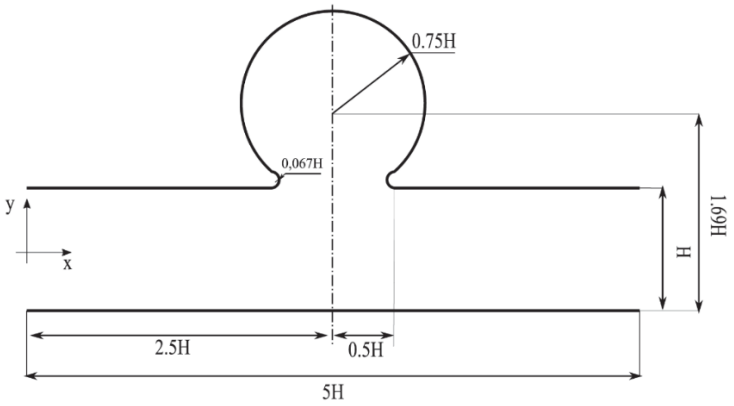

Figure 4. Idealized aneurysm geometry [26].

Assuming that the diffusion of factors was negligible, the concentration of coagulation factors was mapped regarding the residence time distribution. The blood flow was modelled as pulsatile due to the heartbeat and was applied at the vessel inlet. Moreover, the flow was considered as laminar, Newtonian and incompressible. Since systole is the moment of the cardiac cycle when there is the greatest inflow of blood, this moment was modelled with a parabolic velocity profile with a maximum velocity of 10 cm/s. From these conditions, the Navier-Stokes equations describing the motion of the blood were

solved to obtain the velocity field within the aneurysm. Numerical discretisation was carried out using second-order finite differences on a Cartesian staggered grid to approximate the derivatives accurately. A semi-implicit, low-storage, three-stage Runge-Kutta scheme was employed to solve the equations time efficiently. It was also modelled using the immersed boundary method to impose that the fluid velocity at the vessel wall was zero.

With the velocity field within the aneurysm obtained, the residence time of the blood particles was integrated following the study of Esmaily-Moghadam *et al*. [38]. The residence time is calculated by integrating the time a particle spends in a specific area, which is influenced by the flow velocity in that area. The spatial distribution of residence time helps to identify areas within the aneurysm where blood tends to stay longer. From the coagulation cascade model obtained above, linear interpolation was applied to map in 2D the concentration of the different factors based on the calculated residence times (see Figure 5). Although the flow was considered Newtonian, due to the fact that the viscosity evolution was available as the thrombus developed, linear interpolation was also applied to map the viscosity based on the residence time.

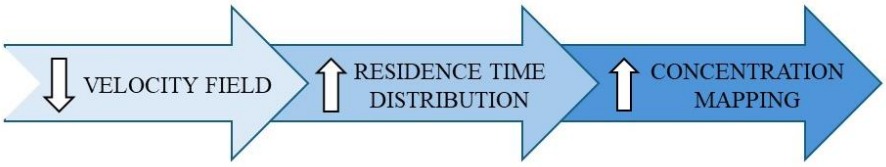

Figure 5. Steps to obtain the concentration mapping in 2D geometry.

2.3.1 Effect of anticoagulant in a 2D aneurysm

The spatial-temporal distribution of coagulation cascade factors when administering an anticoagulant was also assessed. Specifically, the model that was applied was the one containing the effect of warfarin, mentioned in Section 2.2. This model was used to the same spatial distribution of residence time as used for the coagulation cascade model, using the 2D geometry of the idealised aneurysm and the same conditions.

3. RESULTS

3.1 0D model of the coagulation cascade

Numerically solving the systems of ordinary differential equations (Equations 1-16) facilitated tracking the temporal evolution of coagulation factors concentrations.

Figure 6 shows the behaviour of factors involved at the beginning of the coagulation cascade belonging to both the extrinsic and intrinsic pathways. As for the complex formed by tissue factor and factor VIIa, these are the only factors considered in the model as belonging to the extrinsic pathway. It can be seen that the concentration of this complex presents an initial peak and then remains constant. As for the intrinsic pathway, the first factor of this pathway is factor XIa, which shows how its concentration decreases over time. However, factor IXa, which depends on both factor XIa and the TF:VIIa complex, shows a growth that is maintained over time from the beginning although at the end of the simulation it begins to decrease. Factor VIII, which is the last factor of the intrinsic

pathway, has a different behaviour than the other factors of the intrinsic pathway, around the first minute it shows a peak and then disappears.

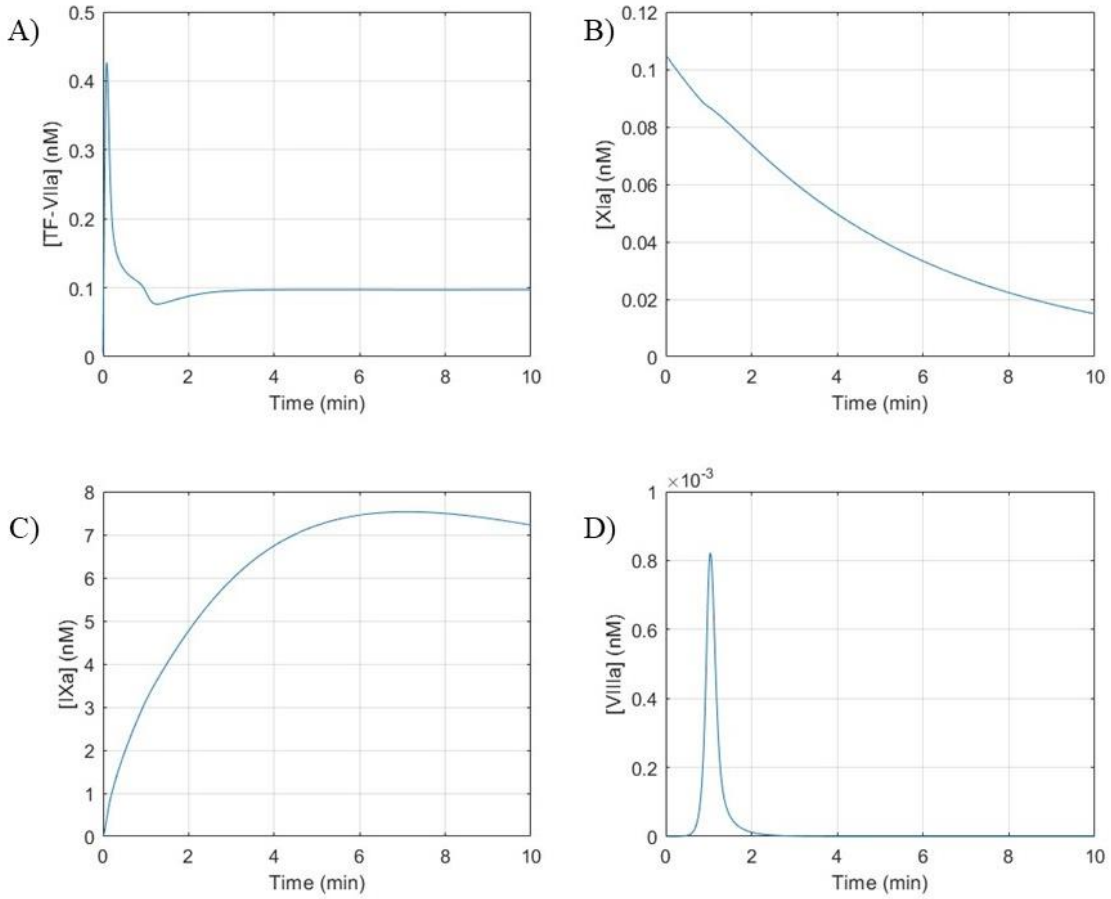

Figure 6. Concentration of procoagulant factors of the intrinsic and extrinsic pathway as a function of time. A) Tissue factor and factor VII complex (TF:VII). B) Factor XI. C) Factor IX. D) Factor VIII. Concentration units are in nanomolar (nM), and time units are in minutes (min).

The behaviour of the coagulation cascade factors that promote thrombus formation and are part of the common pathway is illustrated in Figure 7. Factor X is the first factor of this pathway, which is activated by factors from both the extrinsic and intrinsic pathways, showing a peak at the beginning of the simulation and stabilizing at a constant concentration. Factor V is activated and degradated in a manner similar to factor VIII and thereby exhibiting analogous behaviour. Prothrombin, the precursor of thrombin, is rapidly degradated within the first few seconds until it disappears.

An insight into the behaviour of coagulation factors involved in the system's inhibition processes is provided in Figure 8. Protein C increases rapidly, reaching its maximum concentration after approximately two minutes, and then progressively decreases. Peptide P, which participates in the production of protein C, also reaches a maximum peak before two minutes and then remains constant over time.

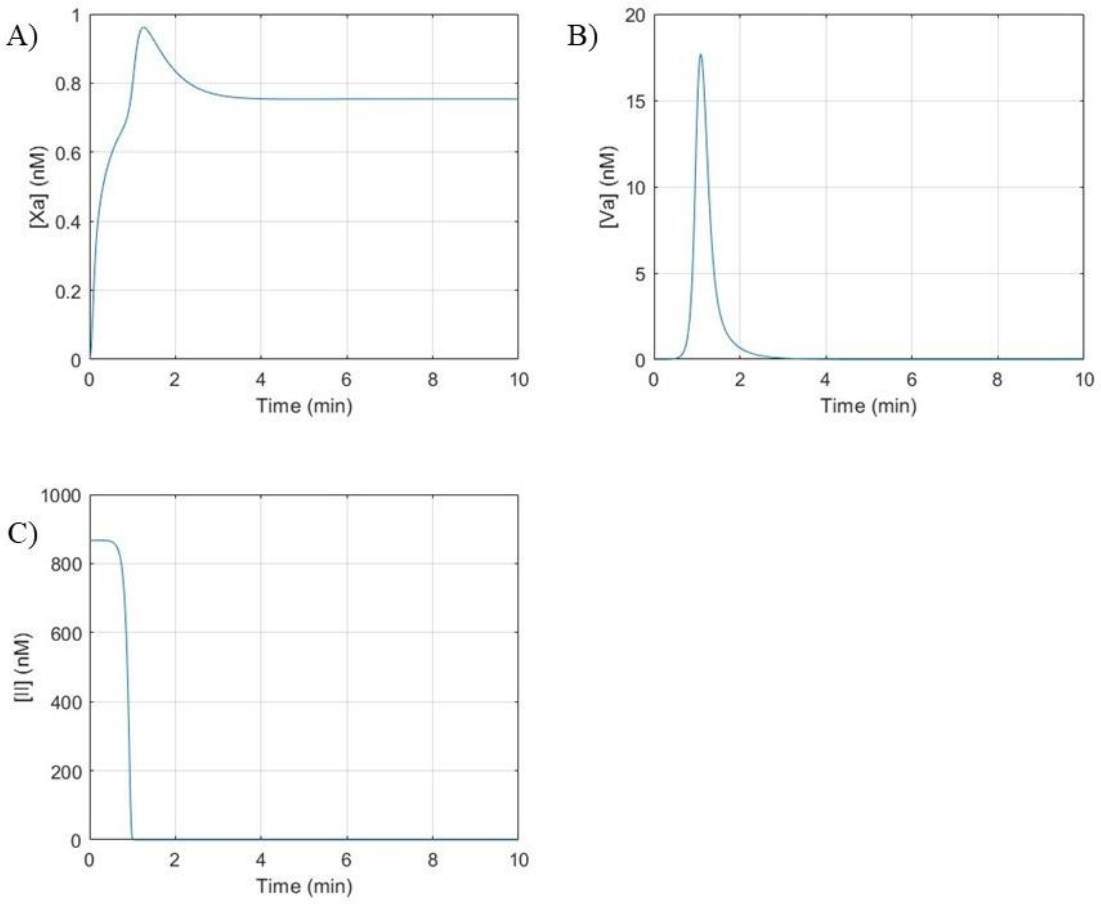

Figure 7. Concentration of procoagulant factors of the common pathway as a function of time. A) Factor X. B) Factor V. C) Prothrombin (factor II). Concentration units are in nanomolar (nM), and time units are in minutes (min).

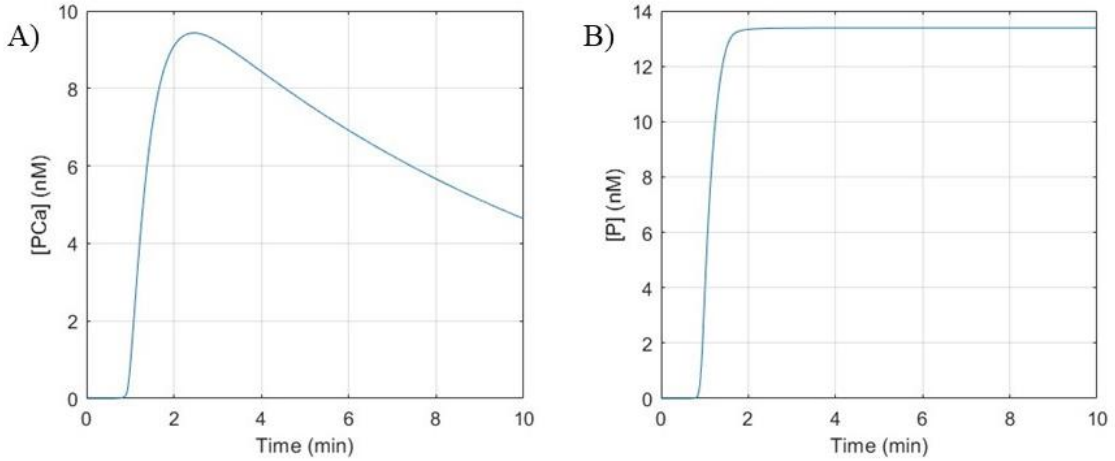

Figure 8. Concentration of the coagulation inhibitors as a function of time. A) protein C (PC). B) peptide P. Concentration units are in nanomolar (nM), and time units are in minutes (min).

As for the behaviour of fibrinogen, which is the precursor of fibrin, the simulation was carried out for 10 minutes; Figure 9 shows the first 2 minutes. In Figure 9 it can be seen that initially only inactivated fibrinogen is present but quickly becomes activated until it reaches its peak before the first minute. Once this maximum concentration has been reached, both the inactive and active fibrinogen degrades until it disappears.

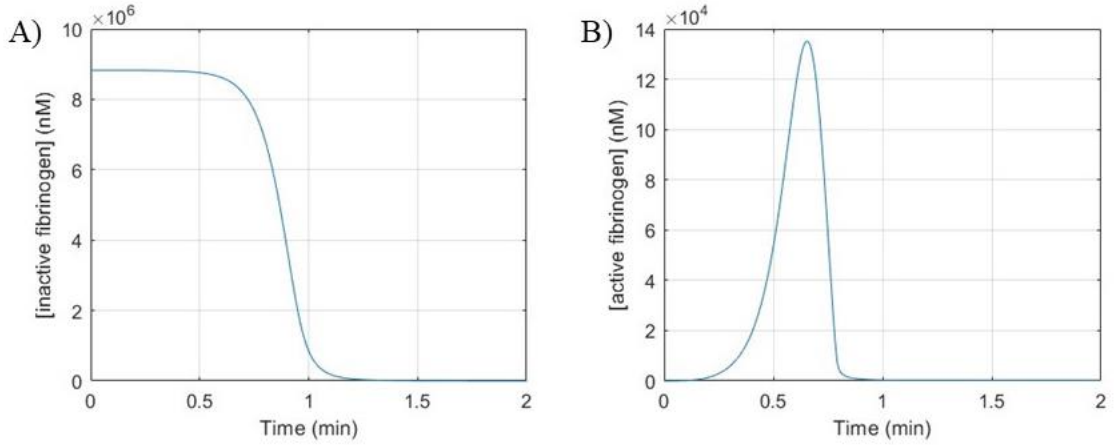

Figure 9. Concentration of fibrinogen as a function of time. A) First two minutes of the inactive fibrinogen. B) First two minutes of the active fibrinogen. Concentration units are in nanomolar (nM), and time units are in minutes (min).

Regarding the behaviour of the key factors in the coagulation cascade, thrombin and fibrin, can be seen in Figure 10. Thrombin takes a few minutes to peak, reaching a maximum concentration of 670.14 nM. It then decreases slower than it has been synthetized until it reaches a concentration close to zero at minute three. As for fibrin, it also takes a few seconds to be activated and increases in concentration until it reaches a maximum concentration of $8.8 \cdot 10^6$ nM where it remains constant over time. The maximum fibrin concentration is reached at the moment when thrombin disappears, around minute three.

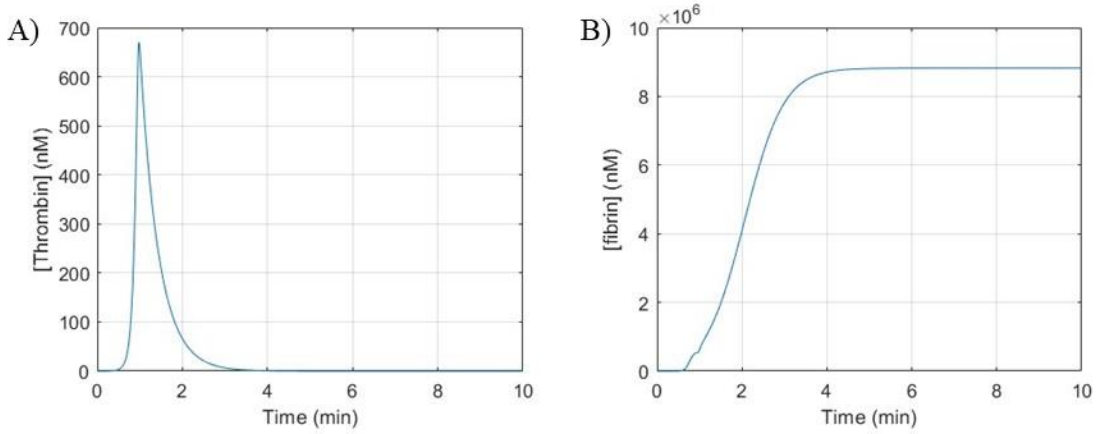

Figure 10. Concentration of thrombin and fibrin as a function of time. A) Thrombin. B) Fibrin. Concentration units are in nanomolar (nM), and time units are in minutes (min).

3.1.1 Viscosity change

In Figure 11, the cooperativity curve is depicted, illustrating viscosity as a function of the ratio of fibrin to fibrinogen, thereby indicating its proportionality to the amount of thrombus being formed. It can be observed that in the absence of thrombus, the viscosity matches the viscosity of blood under regular conditions. As the ratio increases, viscosity does so.

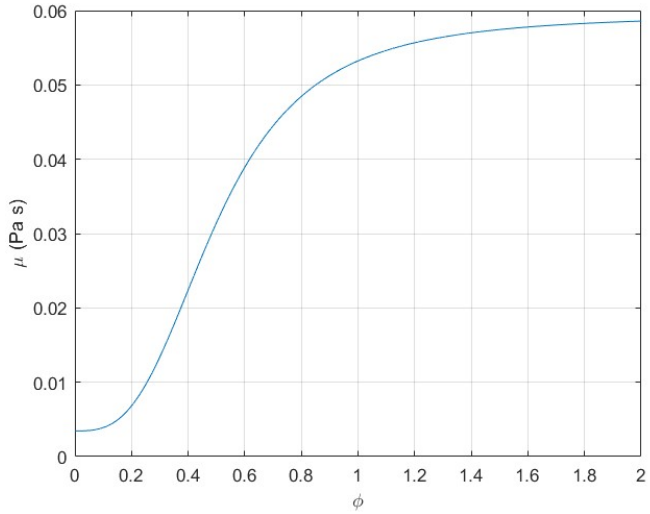

Figure 11. Cooperativity curve. Viscosity (μ) as a function of the ratio of fibrin to fibrinogen (ϕ).

3.1.2 Sensitivity analysis

The targeted parameters on which the action of varying initial conditions was analysed were: the maximum peak thrombin concentration, the time between the thrombin peak and its disappearance and the final fibrin concentration. The distribution of the results can be seen in Figure 12. Regarding the maximum concentration of thrombin, it ranged from 747.45 to 1.26×10^3 nM depending on the initial concentrations. The time from the peak to the disappearance of thrombin varied between 3.41 and 3.18 minutes. Finally, the final concentration of fibrin ranged from 8.8233×10^6 to 8.8228×10^6 nM.

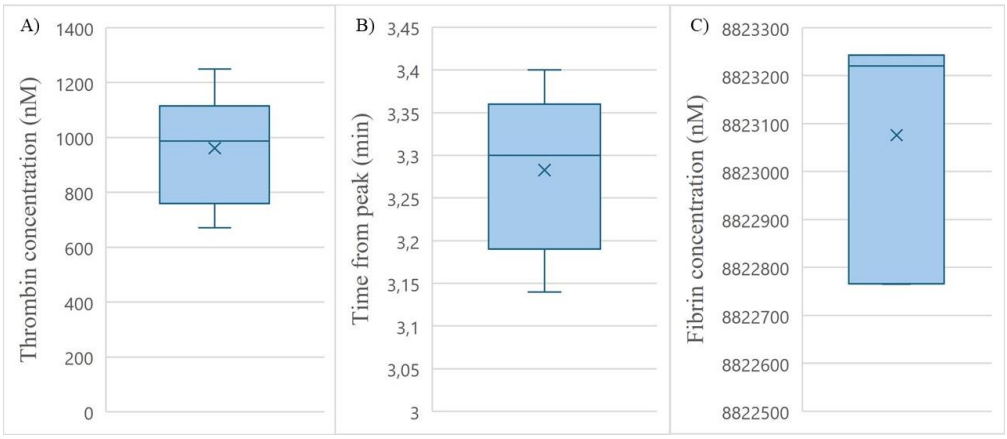

Figure 12. Results distribution. A) Maximum thrombin concentration. B) Time from the peak to the disappearance of thrombin. C) Final fibrin concentration. Concentration units are in nanomolar (nM), and time units are in minutes (min).

The most important factors for each targeted parameter are shown in Figure 13. Prothrombin was the most important factor affecting all parameters studied. Another important factor, although to a lesser extent, was factor XI, which affects thrombin-related parameters, both peak concentration and time to disappearance significantly (α=0.05). The same was not true for the fibrin parameter which, although affected by factor XI, is not significantly influenced (α=0.05). TF was not significantly affecting the final activation level of the studied parameters (α=0.05). The p-value for each parameter can be seen in Table 6 in S.3.

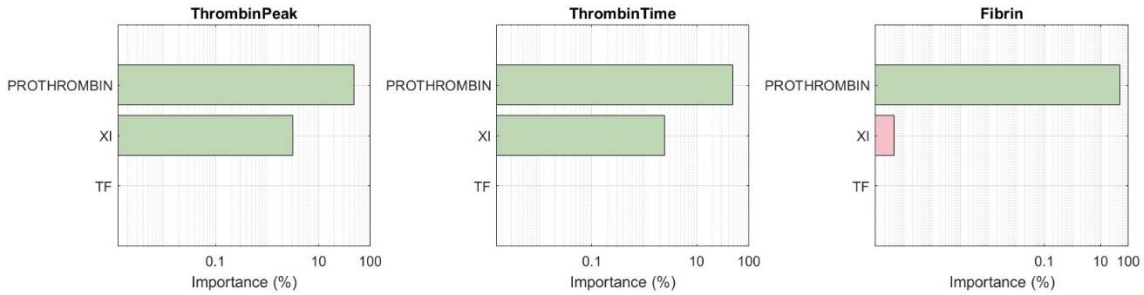

Figure 13. Bar chart showing the importance of each factor with respect to each parameter. Significant results are shown in green (α=0.05) and non-significant results in pink.

3.2 Effect of anticoagulant

The effect of warfarin was applied to the coagulation cascade model. The impact of this anticoagulant was studied for 10 minutes. The plasma concentration of warfarin was found to be maximal initially and decreasing over time, as shown in Figure 24 in S.4.

The effect of warfarin on the coagulation cascade model is shown in Figure 14. There is hardly any difference in factor XIa between the model with and without warfarin. Warfarin affects both the TF:VIIa complex and factor IXa, so it is observed that the model containing warfarin has a lower concentration than that obtained in the model without anticoagulant. As for factor VIII, its production is delayed in the warfarin-containing model. However, this factor reaches a higher concentration when the anticoagulant is applied.

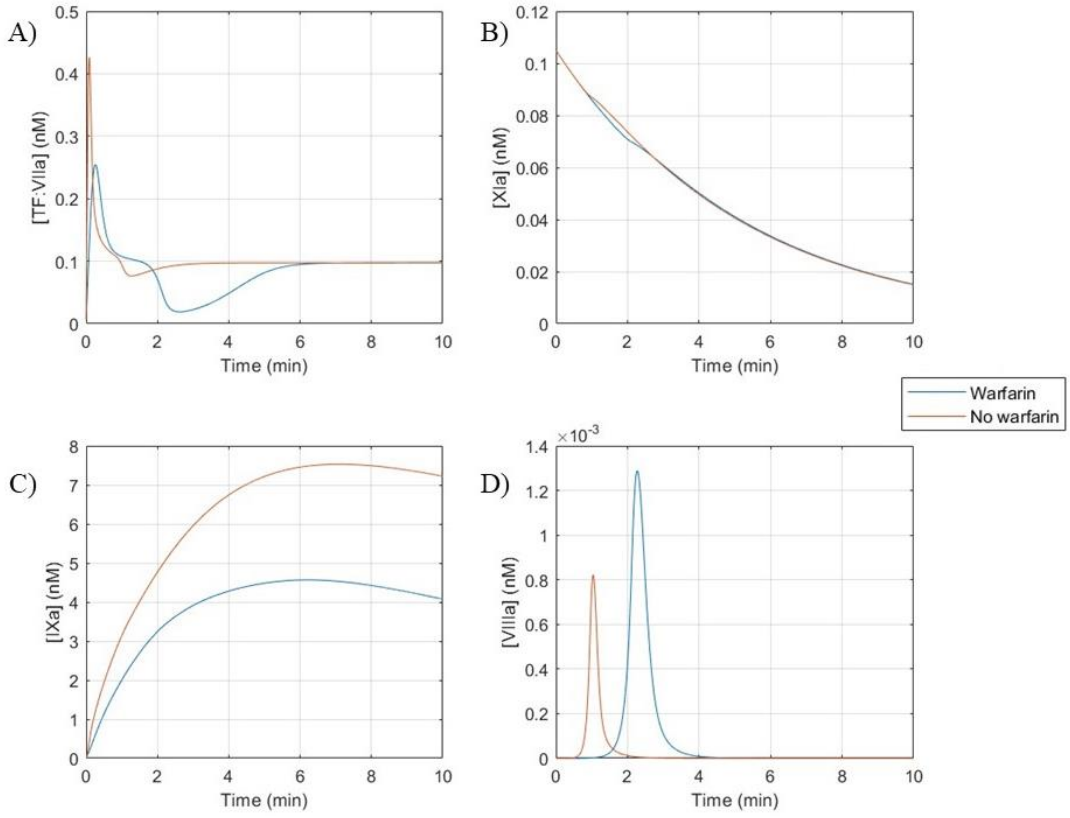

Figure 14. Concentration of procoagulant factors of the extrinsic and intrinsic pathway as a function of time with and without warfarin. A) Tissue factor and factor VIIa complex

(TF:VIIa). B) Factor XIa. C) Factor IXa. D) Factor VIIIa. Concentration units are in nanomolar (nM), and time units are in minutes (min). The blue line represents the model with warfarin and the orange line represents the model without warfarin.

The degradation of factor VIII depends on protein C, which is one of the targets of warfarin and therefore its concentration is reduced (Figure 15). The peptide P also presents a reduction in its concentration.

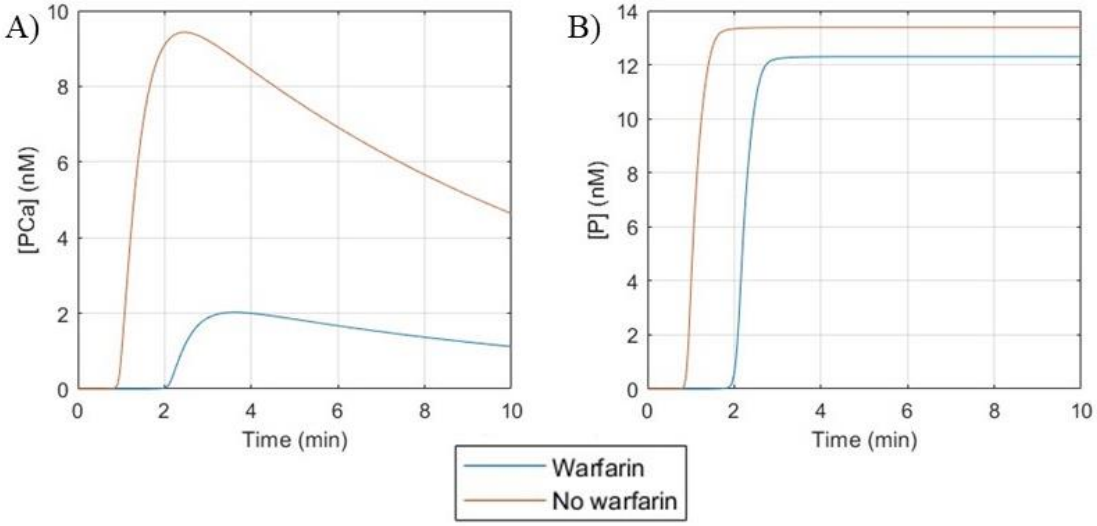

Figure 15. Concentration of the coagulation inhibitors as a function of time with and without warfarin. A) protein C (PC). B) peptide P. Concentration units are in nanomolar (nM), and time units are in minutes (min). The blue line represents the model with warfarin and the orange line represents the model without warfarin.

The behaviour of some common pathway factors is illustrated in Figure 16. Factor X shows a reduction in its concentration because the anticoagulant directly affects this factor. In addition, the production of this factor depends on factors of the extrinsic and intrinsic pathway that have been affected by the anticoagulant. Factor V has the same behaviour as factor VIII. Factor V production is delayed but reaches a higher concentration in the anticoagulant model. Prothrombin is directly affected by warfarin, and a delay in its degradation is observed.

Regarding the behaviour of fibrinogen, although the simulation was carried out for 10 minutes, Figure 17 shows the first 3 minutes. The effects produced by warfarin on different factors of the coagulation cascade eventually affect fibrinogen activation. The effects are observed with delayed activation and decreased magnitude.

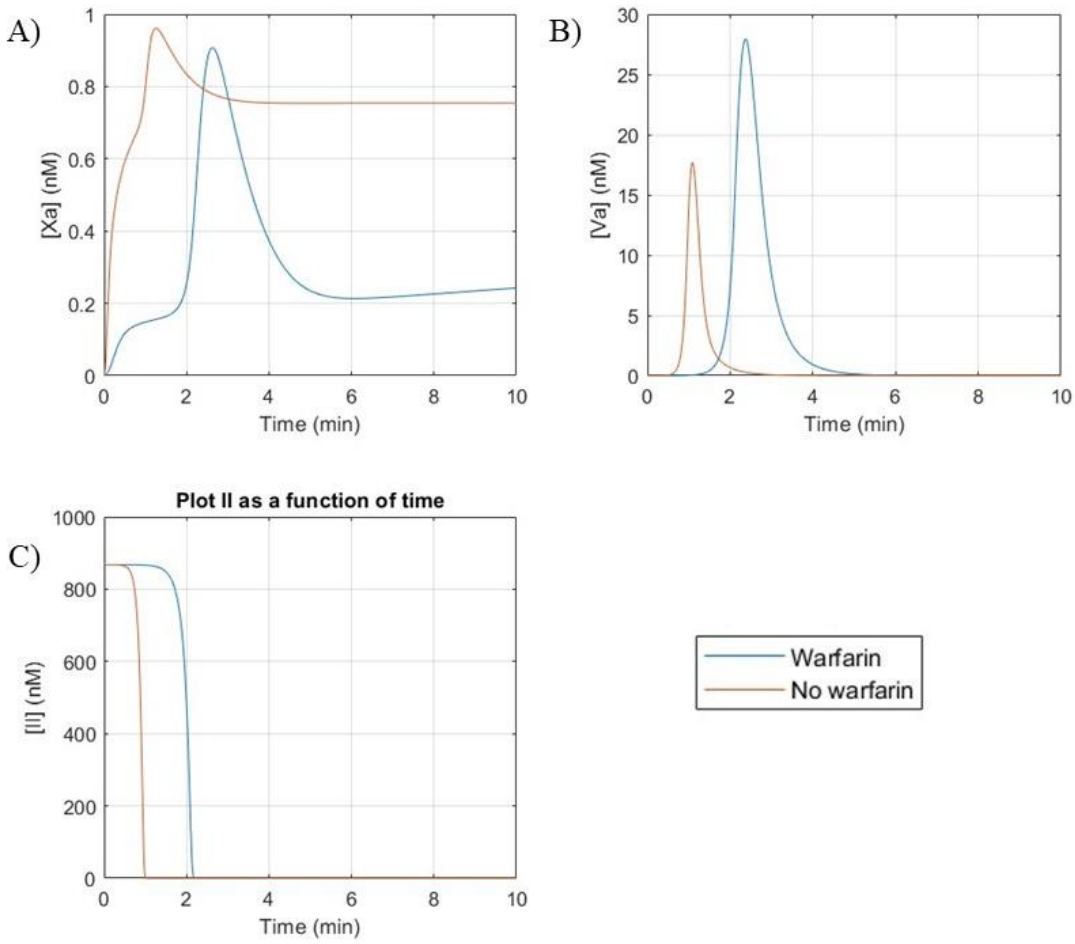

Figure 16. Concentration of factors of the common pathway as a function of time with and without warfarin. A) Factor X. B) Factor V. C) Prothrombin (factor II). Concentration units are in nanomolar (nM), and time units are in minutes (min). The blue line represents the model with warfarin and the orange line represents the model without warfarin.

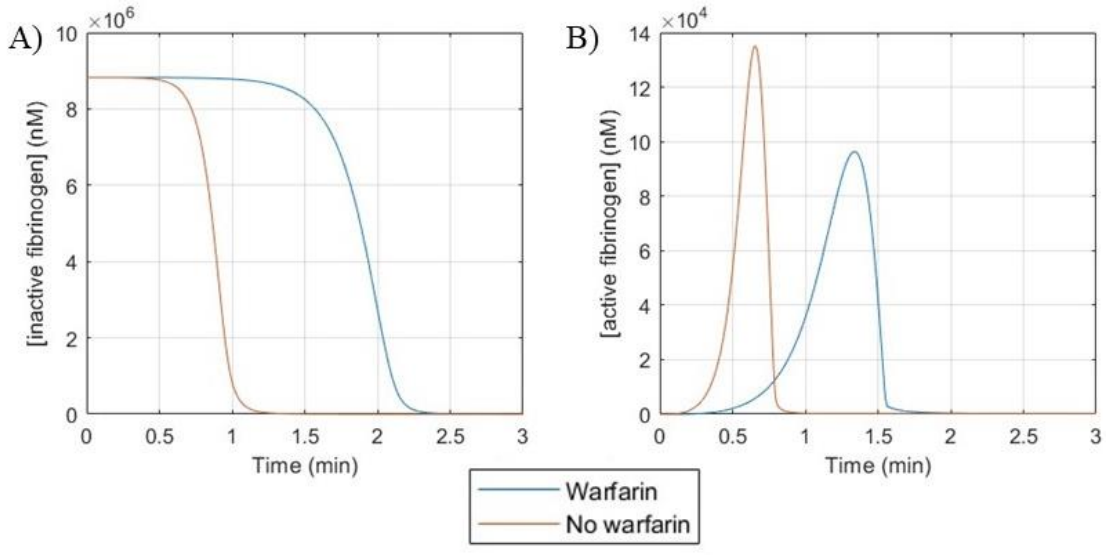

Figure 17. Concentration of fibrinogen as a function of time with and without warfarin. A) First three minutes of the inactive fibrinogen. B) First three minutes of the active

fibrinogen. Concentration units are in nanomolar (nM), and time units are in minutes (min). The blue line represents the model with warfarin and the orange line represents the model without warfarin.

As for the behavior of both thrombin and fibrin, which are key factors in the coagulation cascade, can be seen in Figure 18. Like many of the previous factors, both show a delay in their production. As for thrombin, it reaches a lower maximum concentration in the case of the model with warfarin, going from 670.14 nM to 591.01 nM. In addition, the time it takes to degrade increases from 2.15 minutes for the model without warfarin to 3.09 for the model with warfarin. As for fibrin, although it takes longer to start production, it ends up reaching the same maximum concentration.

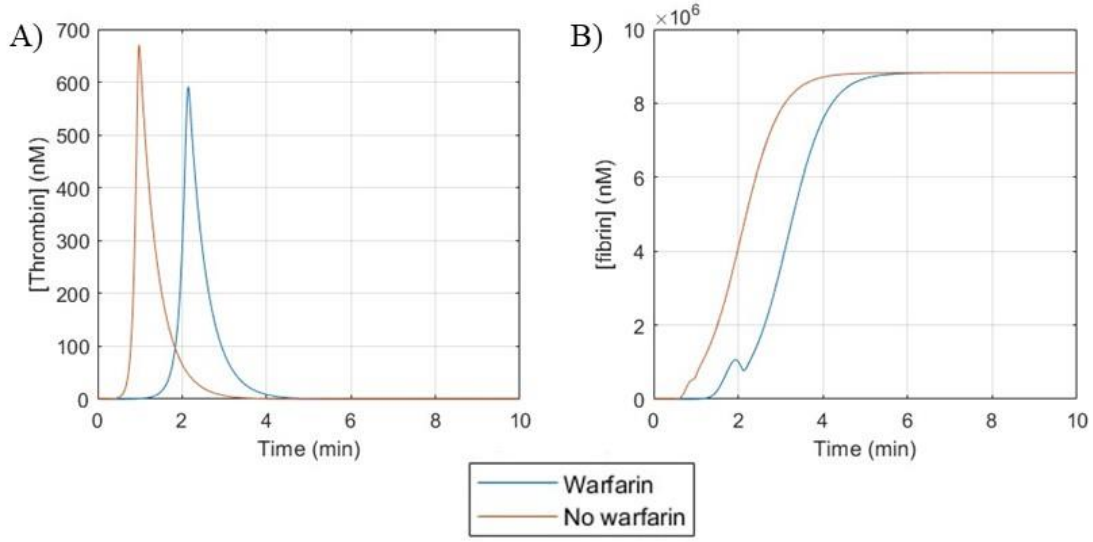

Figure 18. Concentration of thrombin and fibrin as a function of time with and without warfarin. A) Thrombin. B) Fibrin. Concentration units are in nanomolar (nM), and time units are in minutes (min). The blue line represents the model with warfarin and the orange line represents the model without warfarin.

3.3 Coagulation cascade in a 2D aneurysm

Since this distribution is the same across all factors, their distributions are very similar, even though the achieved concentrations vary. Therefore, as a pulsatile inflow has been defined, an acceleration and a deceleration phase can be observed when looking at the spatial-temporal distribution of the coagulation factors.

In the case of fibrin, it can be seen in Figure 19 that the highest concentration of the coagulation factor is found in the interior of the aneurysm, which is the region with the slowest velocity. In contrast, the vessel, which is a region where the flow velocity is not affected, has a low fibrin concentration. Regions with lower velocities have a longer residence time, which leads to an increase in the concentration of coagulation factors. Since the flow velocity in the wall is zero, these areas present a higher fibrin concentration, as can be seen in Figure 19D. Furthermore, it can be observed how the distribution of fibrin is affected by the acceleration and deceleration phases of the flow. Figure 19A and 19C shows two different times but both are in the deacceleration phase, which causes blood flow to enter from the part of the aneurysm neck most distal to the flow inlet. This causes a flow of blood with a low concentration of fibrin to enter the aneurysm, causing a flow of blood with a higher concentration of fibrin to flow out into the vessel. Following this phase, acceleration occurs, which is observed in both Figure

19B and 19D. In this phase, the inflow is at its maximum, causing the flow with high concentration of fibrin that has left the aneurysm to mix with the vessel flow and disappear. The fact that the deacceleration phase causes the inflow with low concentration to enter the aneurysm from the distal part of the aneurysm neck and the outflow with high concentration to exit to the vessel from the proximal part of the aneurysm neck, generates counterclockwise vortices inside the aneurysm. Thus, as time progresses, the concentration of fibrin within the aneurysm increases and vortices are present, this can be seen in Figure 19C and 19D.

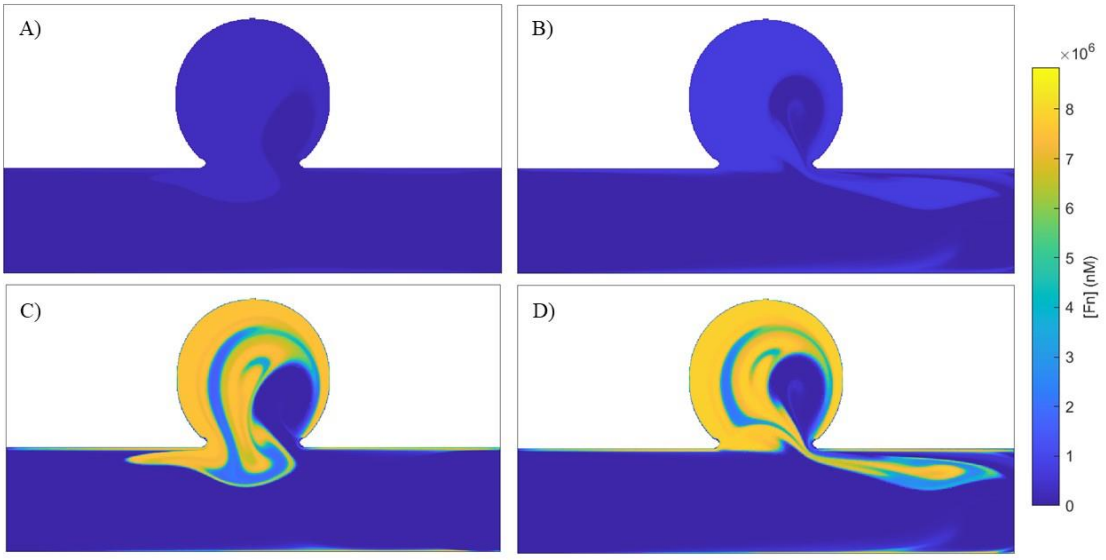

Figure 19. Fibrin (Fn) concentration distribution in the 2D geometry of an aneurysm. A) Second 24.17 of the simulation. B) Second 32.22 of the simulation. C) Second 90.23 of the simulation. D) Second 95.06 of the simulation. Concentration units are in nanomolar (nM).

In all coagulation factors it can be observed that, at a certain point in the simulation, there is a noticeable difference between the concentration of clotting factors inside the aneurysm and in the blood vessel. In addition, the effect of pulsatile flow is also apparent. It can be seen how blood flows in and out of the aneurysm through the same region: one flow of blood enters the aneurysm, and another flow exits into the vessel. As the simulation progresses, counterclockwise vortices are generated, the intensity of which varies according to the clotting factor (Figure 25 in S.5). It should be noted that the concentrations achieved vary depending on the coagulation factor. Regarding the precursors of some of the factors in the coagulation cascade, such as prothrombin or fibrinogen, the opposite is observed for the other factors. In these cases, they are found in high concentration in the vessel and in low concentration inside the aneurysm, especially as the simulation progresses (Figure 26 in S.5).

As for the viscosity (Figure 20), at second 33.03 the maximum viscosity is reached both inside the aneurysm and in the vessel wall, since these are sites that present lower velocity, so the coagulation cascade is triggered, producing this increase in viscosity. As for the inside of the vessel, because the blood flow is not affected, it has a viscosity closer to zero, which is considered as the viscosity of blood under normal conditions.

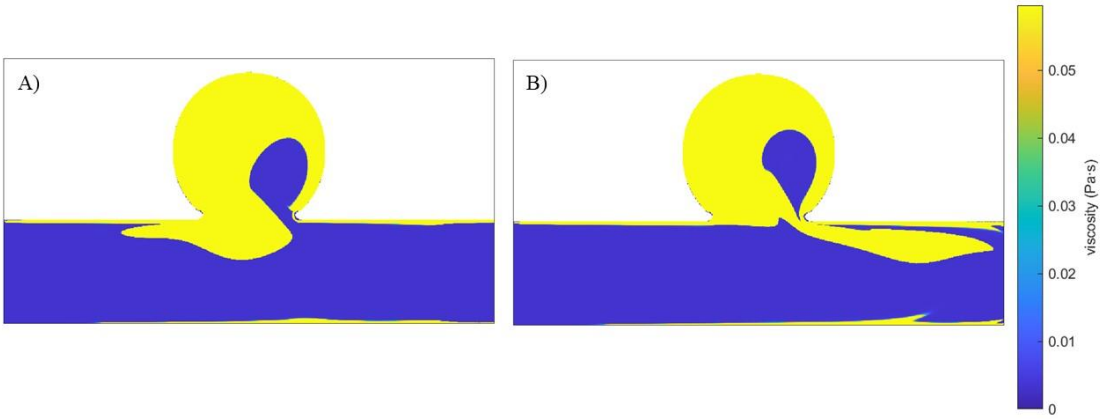

Figure 20. Viscosity distribution in the 2D geometry of an aneurysm. A) Second 90.23 of the simulation. B) Second 95.06 of the simulation. Units are in pascal-second (Pa·s).

3.3.1 Effect of anticoagulant in a 2D aneurysm

The model of the coagulation cascade with anticoagulant shows similarities to the model without anticoagulant. For all coagulation factors, it can be seen that at a certain point in the simulation there is an inflow into the aneurysm and an outflow into the vessel. In addition, as the simulation progresses, counterclockwise vortices can be observed. In most coagulation factors a higher concentration is found inside the aneurysm than in the vessel (Figure 27 in S.6). The opposite occurs in factors that are precursors such as prothrombin or fibrinogen (Figure 28 in S.6). It should be noted that warfarin does not completely prevent the formation of clotting factors, but it does reduce their concentrations and their time to form.

When warfarin is applied, the production of coagulation factors is delayed, this can be observed in the case of fibrin in Figure 21. In second 41.89, in the case without warfarin it could already be seen that fibrin was being produced (Figure 21A), this does not occur in the case with warfarin (Figure 21B). As the simulation progresses (Figure 22), it can be noticed that fibrin is being produced inside the aneurysm. When comparing the same frame of fibrin and warfarin concentration distribution, it can be observed that in the area where the anticoagulant has reduced its concentration is the same area where fibrin has begun to form (Figure 22B, Figure 29 in S.6).

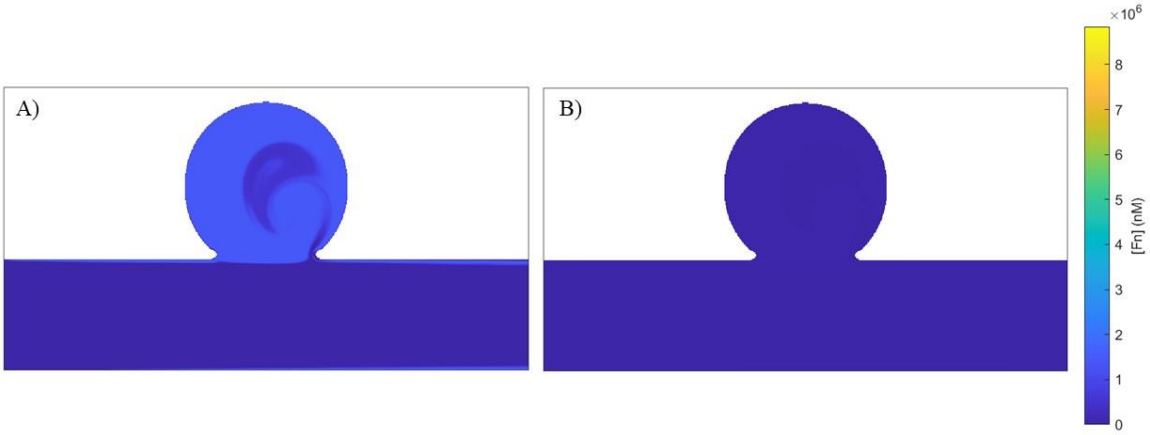

Figure 21. Fibrin (Fn) concentration distribution in the 2D geometry of an aneurysm in the second 41.89 of the simulation. A) Without warfarin. B) With warfarin. Concentration units are in nanomolar (nM).

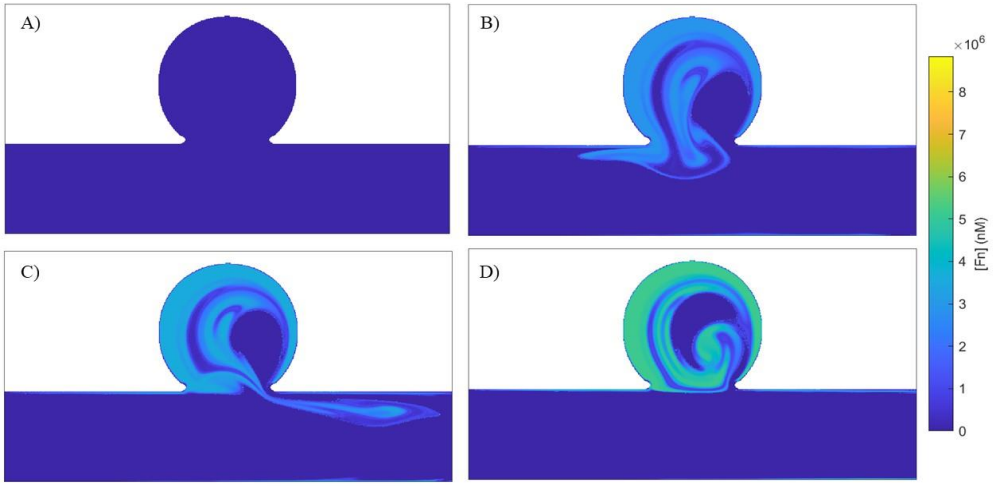

Figure 22. Fibrin (Fn) concentration distribution in the 2D geometry of an aneurysm with warfarin. A) Second 32.22 of the simulation. B) Second 90.23 of the simulation. C) Second 95.06 of the simulation. D) Second 105.53 of the simulation. Concentration units are in nanomolar (nM).

As for viscosity (Figure 23), something similar to what happened with fibrin occurs. A delay in its increase it is observed. In addition, the area with the highest viscosity is the area with the highest concentration of fibrin and, therefore, has the lowest concentration of warfarin.

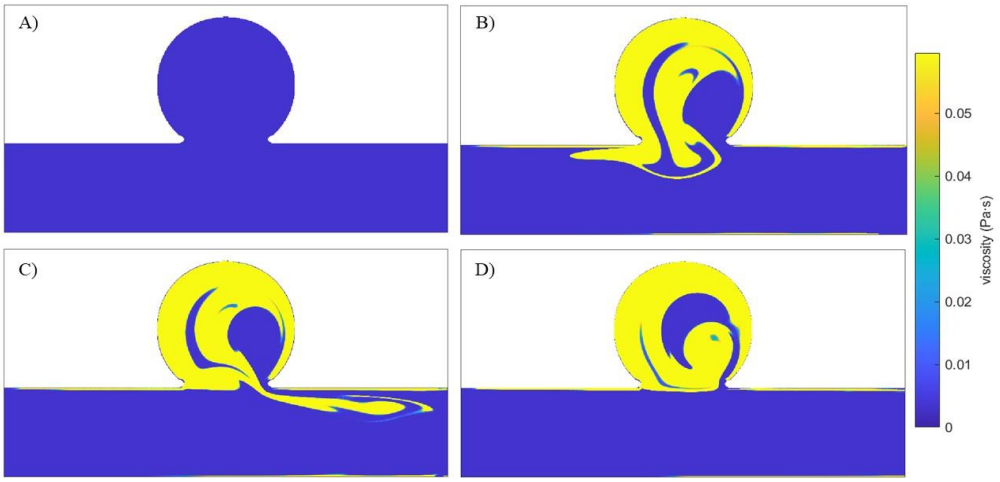

Figure 23. Viscosity distribution in the 2D geometry of an aneurysm with warfarin. A) Second 32.22 of the simulation. B) Second 90.23 of the simulation. C) Second 95.06 of the simulation. D) Second 105.53 of the simulation. Units are in pascal-second (Pa·s).

4. DISCUSSION

The main objective of this work was to model the coagulation cascade to study thrombus formation. There are a variety of models in the literature describing the coagulation cascade, but in many studies the coagulation cascade is studied separately [19, 20, 29, 33]. In contrast, this work presents a simplified model that couples all the pathways of the coagulation cascade.

Analysing the behaviour of the different coagulation factors of the model, it can be observed that factor XI is decreasing in concentration but is still in sufficient quantity to activate factor IX. Since in this model factor XI formation only depends on thrombin, the strong peak observed in this factor is sufficient to induce enough XI concentration in a feedforward loop which would contribute to clot formation. This was demonstrated experimentally by Naito *et al*. [39].

The factor IX, the TF:VII complex and factor X increase their concentration at the beginning until they reach a point where they stabilize. The presence of an initial peak of TF:VII complex is explained by the fact that this complex is principally responsible for the initial production of thrombin which allows the generation of an unstable clot [40]. Therefore, a quick response to an injury might help to stop the bleeding. Thrombus growth is more related to the intrinsic pathway [40], for this reason factor IX has a slower growth. As for factor X, it represents a key activator of prothrombin and therefore presents an increase in its concentration at the beginning. Due to its role in the cascade, many anticoagulants interfere with this factor [41].

As for factor VIII and V, both present the same behaviour, which consists of a peak, this is because it is assumed that they undergo the same degradation since both are inhibited in the same way by protein C. Since deficiency of these factors is associated with mild symptoms [42], this suggests that their transient peaks are sufficient to maintain adequate haemostasis. This indicates that the regulatory mechanisms involving protein C are effective in modulating the activity of factors VIII and V, ensuring adequate thrombus formation without leading to excessive coagulation.

As for the precursors, it is observed that when the concentration of prothrombin decreases, the concentration of thrombin begins to increase. In the case of fibrinogen the same thing happens, at the moment that all the fibrinogen has been activated, it is converted into fibrin. In terms of thrombin behaviour, it exhibits the characteristic ‘lag’ phase of the thrombin generation profile [43]. During the initiation phase, so little thrombin is produced that it is not detectable, resulting in this delay in thrombin production [43]. Following this phase, thrombin presents a peak, which is consistent with what occurs in the propagation phase of the coagulation cascade. In this phase, sufficient clotting factors have been generated in both the extrinsic and intrinsic pathways to cause thrombin formation [7]. There comes a point at which the thrombin concentration reaches its maximum and begins to decrease. This is because thrombin production and inhibition reach an equilibrium [43], which is also when TFPI begins to inhibit thrombin.

Arguably, the maximum thrombin concentration reached is higher than what was expected, and the peak time is shorter. This might be explained because the equations for the intrinsic and common pathway factors up to thrombin formation (Equations 2-10) come from a model [19] that did not include the extrinsic pathway. In order to develop the model of this work, terms referring to the extrinsic pathway have been added from Xu *et al*. [7]. In fact, the maximum concentration reached by our model (i.e., 670.14 nM) is higher than reported thrombin concentrations in the literature, which is approximately 377 nM [44]. Thus, this model might overestimate thrombin concentration leading to smaller ‘lag’ phases, which is characteristic of a state with high hypercoagulability. Thrombus formation occurs at the end of the ‘lag’ phase [45]. Comparing the behaviour of thrombin with that of fibrin it can be seen that it is at the end of this phase that fibrin starts to be generated. Moreover, this is not the only relationship between thrombin and fibrin, the concentration of thrombin affects the structure of fibrin, since it mediates the

conversion of fibrinogen to fibrin. If thrombin concentration is low, the fibrin fibres will be thick and highly permeable, making them susceptible to fibrinolysis [46]. Fibrin is the final product of the coagulation cascade, which provides information about the development of the thrombus [45]. Since a high concentration of thrombin has been obtained in this model, it suggests that fibres more resistant to fibrinolysis might be produced, generating a more stable thrombus.

As for viscosity, when the thrombus has not been developed or is still very small, the viscosity is the same as that found in the blood under normal conditions, since the blood is in a liquid state. As the thrombus grows, the blood in that region rapidly shifts to a solid state of aggregation, as seen in Figure 11. Our system can only be found in one of the two steady states, so it cannot be found in a semi-liquid state, as other studies postulate [47, 48].

The sensitivity analysis allowed the evaluation of three of the factors that are present at the beginning of the coagulation cascade, namely tissue factor, factor XI and prothrombin. Their effects were evaluated on three parameters related to thrombus formation, specifically the maximum thrombin concentration, the time between the thrombin peak and its degradation and the maximum fibrin concentration. The results show that prothrombin is a crucial factor in the coagulation cascade, with a strong influence on thrombin and fibrin formation. The results are coherent since the conversion of prothrombin to thrombin is a crucial step in the coagulation cascade. Once prothrombin has been converted to thrombin, there is no way back to stop the cascade. This process is irreversible, ensuring that the coagulation cascade progresses in a unidirectional manner. In addition, thrombin has the ability to amplify its signal through a positive feedback mechanism. This mechanism of thrombin ensures that coagulation expands rapidly, increasing the efficiency of the process [3]. It should also be noted that prothrombin is a factor that many anticoagulants interfere with, which demonstrates the importance of this factor in thrombus formation [40].

Factor XI influences thrombin formation (Figure 13). Although it also affects fibrin formation, its impact is not significant (Figure 13). This is because it is the first factor of the intrinsic pathway in the model. Factor XI has an indirect effect on thrombin formation, as it participates in the production of other factors that ultimately lead to thrombin formation. Although the effect of factor XI is not as relevant as that of prothrombin, it represents a potential target for anticoagulation. Several factor XI inhibitors have successfully completed phase 2 clinical trials [40, 49].

Finally, the tissue factor has no significant impact on the behaviour of the model. It has no significant influence on either thrombin or fibrin production. This may be due to several causes. The complex formed between tissue factor and factor VII is the only one of the extrinsic pathway that has been considered in the model. This complex indirectly leads to thrombin formation through the activation of other factors that are also activated by the intrinsic pathway. It is important to note that the extrinsic pathway is more involve in the initiation of the coagulation cascade, whereas the intrinsic pathway plays a more significant role in thrombus growth and stabilization. Since the parameters studied are more related to the latter aspects than to initiation, this might explain the lack of a significant impact of tissue factor [40]. In addition, human platelets have been shown to supply tissue factor, and platelets are not considered in this model, which may be contributing to the underestimation of the tissue factor effect [50].

In terms of the effect of warfarin on the coagulation cascade model, a remarkable reduction in the concentration of the TF:VII complex, factor IX and factor X is observed. This is because warfarin has a direct effect on these factors by inhibiting its principal cofactor, vitamin K. As for factor XI, since it is the first factor of the intrinsic pathway of the model and depends only on the thrombin concentration, it hardly shows changes with the anticoagulant. Contrary, factor VIII and V, are indirectly affected by warfarin as it inhibits the production of TF:VII complex, factor IX, factor X, prothrombin and protein C, leading to delayed production of both factor VIII and V. Arguably, a higher concentration of these factors is obtained in the presence of warfarin. This is because warfarin, besides inhibiting factors involved in thrombus formation, also inhibits protein C. This protein plays an important role in the degradation of factors VIII and V, so protein C reduction produces an increase in the concentration of these factors. The fact that in our model warfarin inhibits protein C may result in longer clot dissolution profiles, with a consequent increased risk of re-thrombosis, which is a behaviour observed when prescribing this anticoagulant [51].

As for the behaviour of thrombin, a delay in its production is observed in the presence of warfarin. This is because prothrombin is also affected by the action of warfarin, causing a delay in the production of thrombin. In addition, thrombin also shows a reduction in its concentration, which has been previously observed in the study of Rigano *et al*., [52] since they showed that when warfarin was administered, the concentration of thrombin was reduced, and its production was delayed. Therefore, the delay in thrombin production leads to a delay in fibrinogen activation, which in turn affects fibrin production, causing a delay in its formation. Despite the evident effect of warfarin in the model, it is not sufficient to prevent thrombus formation, since the fibrin concentration reached at the end of the simulation is the same as that reached in the model without anticoagulant. Throughout the simulation warfarin concentration is within the therapeutic range [37]. However, warfarin has been considered to affect equally all the coagulation factors on which it acts. This may lead to excessive inhibition of protein C, which in turn favours thrombus formation. In addition, the way in which warfarin acts on the coagulation cascade is more complex than what has been considered in the model. This anticoagulant does not act directly on the coagulation factors but inhibits the reduction reactions of the vitamin K cycle, ultimately leading to a decrease in the synthase of vitamin K-dependent factors. Finally, another potential factor is that the model is in a hypercoagulable state, so warfarin, is not able to prevent thrombus formation.

In addition, mapping in a 2D geometry, coagulation factors provide insight into possible regions in which a thrombus could form. Therefore, this study mapped the distribution of coagulation factors based on Guerrero-Hurtado *et al.*, [26] methodology. However, authors in [26] only mapped the intrinsic pathway. The geometry used was an idealised aneurysm, since it is a cardiovascular structure associated with thrombosis. As for the results obtained with the coagulation cascade model in the 2D geometry, a slight inflow into the aneurysm and an outflow into the vessel are observed. In addition, this behaviour causes vortices as well as an increase in the concentration of factors favouring thrombus formation inside the aneurysm. The observed flow follows the same pattern as that of the study of Guerrero-Hurtado *et al.*, [26], as both studies have the same blood flow conditions defined. As the simulation progresses, the concentration of these factors increases in the area where blood accumulates, leading to a possible thrombus formation in such region. In addition, precursors such as prothrombin and fibrinogen show higher concentrations at the beginning of the simulation, and as time progresses, the region where they show lower concentrations is the region where the blood pools. This is because

it is in this area where the highest concentration of prothrombin and fibrinogen is converted into thrombin and fibrin. The fact that the thrombus develops inside the aneurysm causes the blood viscosity to increase in that region. It should be noted that since the system must be in one of the two steady states, liquid or solid, it moves quite fast from normal blood viscosity to maximum viscosity.

Adding the effect of warfarin to the model of the coagulation cascade in the 2D geometry of the aneurysm shows both a delay in the appearance of the different coagulation factors and a reduction in the concentrations reached. As mentioned above, the coagulation cascade model with warfarin is not able to completely prevent thrombus formation. However, it is in the region where the concentration of the warfarin is lowest that the highest concentration of factors favouring thrombus formation is observed.

Considering platelet activation could help to obtain a more realistic model, since they play an important role in thrombus formation. Several CFD models have been developed that consider coagulation reactions in addition to platelet activation [53, 54]. In a study by Rezaeimoghaddam *et al*., [53] the finite volume method was employed to assess thrombus growth. Platelet activation and aggregation were considered to predict the shape and size of the thrombus in the vascular injury region. To do so, convection-diffusion-reaction equations were applied in a tube. A study by Shankar *et al*., [54] developed a 3D multiscale model to predict thrombus growth. The simulation was conducted in a microfluidic device and in a cylindrical tube in the presence of collagen and tissue factor. Additionally, platelet signalling was also considered, and its position was tracked.

The model has several limitations. Firstly, it does not take into account the role of platelets, which play an important role in thrombus development. It also assumes a limited amount of tissue factor, with all available tissue factor forming a complex with factor VII, which rapidly self-activates. Additionally, the model considers only 10 minutes, whereas anticoagulants typically have an action time of hours. Warfarin has been considered to have a direct effect on the clotting factor it affects, rather than its indirect effect via vitamin K. In the simulation of the aneurysm model, the flow rate at an instant does not capture the full complexity of how that flow varies over time in the way that full physiological waveforms would. Lastly, the kinetic reactions are slower than the cardiac cycles, which means that long simulations are required.

Future work could involve several improvements and extensions to improve the realism and applicability of the model. Incorporating the effect of the platelets would provide a more accurate representation of thrombus development. To better simulate the effect of warfarin, the vitamin K cycle should be included, since warfarin inhibits the reduction reactions in the vitamin K cycle. Additionally, models could be carried out with other anticoagulants or antiplatelet agents, if the action of platelets is modelled accordingly. Coupling the coagulation cascade model with a 3D fluid simulation of the left atrium, including the appendage, would provide a more comprehensive understanding of the hemodynamic environment and its influence on clot formation. Finally, a study could be made of how the velocity and geometry of the aneurysm affect the increase in viscosity.

5. CONCLUSIONS

The main objective of this work was, firstly, to develop a computational model of thrombus formation and secondly, to model the influence of anticoagulants when combined with thrombus formation.

In relation to the first objective, a model was developed that captures the critical steps of the coagulation cascade. This allows to track the temporal evolution of coagulation factor concentrations. Although the results suggest that the model is in a state of high hypercoagulability, it is able to describe the expected behaviour of the different factors. In addition, the change in viscosity that occurs as the thrombus develops was described. The viscosity is low in the absence of thrombus, similar to that of blood under normal conditions. However, this viscosity increases rapidly as the thrombus forms, reaching a maximum level.

The influence of tissue factor, factor XI and prothrombin on thrombus formation was also analysed. Specifically, the maximum thrombin concentration, the time between the thrombin peak and its degradation and the maximum fibrin concentration were analysed. It was observed that prothrombin is a crucial factor in the coagulation cascade as it is the precursor of thrombin. Factor XI has less influence as it does not have such a direct action on thrombin and fibrin formation. Finally, tissue factor showed no significant impact. This may be due to the fact that this factor has a more relevant role in the initiation of the cascade than in its propagation, so its effect is not observable in the parameters analysed. It may also be because the model does not consider platelets, which contribute to supplying tissue factor.

The spatial-temporal distribution of both cascade factors and viscosity in an idealised two-dimensional aneurysm was also evaluated. From the residence time of the blood flow, the concentration of the different coagulation factors was mapped. Higher concentrations of coagulation factors were observed within the aneurysm, and these concentrations increased during the simulation. Since the inflow was considered pulsatile, a pattern of inflow and outflow of blood was observed inside the aneurysm causing vortices. In addition, similar behaviour was observed when studying viscosity. All these observed aspects are related to the formation of a thrombus inside the aneurysm.

With respect to the second objective, the effect of warfarin on the coagulation cascade was modelled. The temporal evolution of the coagulation factors after the effect of the anticoagulant was studied and a reduction in both the concentration and activation time of most factors was observed. However, its effect was not sufficient to prevent thrombus formation since the same final fibrin concentration was reached as in the case without anticoagulant. This may be due to the high hypercoagulable state of the model or because the warfarin model is not able to capture all the complexity it presents.

In addition, the spatial-temporal distribution of coagulation factors was also evaluated with the effect of warfarin in an idealized 2D aneurysm. In this case, a reduction in the maximum concentration reached was also observed, as well as a delay in the activation of the coagulation factors. The area with the highest concentration of coagulation factors was the one with the lowest concentration of warfarin, which demonstrates its effect.

In conclusion, this study has provided a basis for realistic simulations in patient-specific geometries in the future to predict thrombus formation and to determine the optimal dose and duration of anticoagulant therapy.

BIBLIOGRAPHY

[1] Furie, B., & Furie, B. C. (2008). Mechanisms of thrombus formation. The New England Journal of Medicine, 359(9), 938–949. https://doi.org/10.1056/nejmra0801082

[2] Alkarithi, G., Duval, C., Shi, Y., Macrae, F. L., & Ariëns, R. A. S. (2021). Thrombus structural composition in cardiovascular disease. Arteriosclerosis, Thrombosis, and Vascular Biology, 41(9), 2370–2383. https://doi.org/10.1161/atvbaha.120.315754

[3] Lippi, G., & Favaloro, E. J. (2018). Venous and arterial thromboses: Two sides of the same coin? Seminars in Thrombosis and Hemostasis, 44(3), 239–248. https://doi.org/10.1055/s-0037-1607202

[4] Huang, T., Li, N., & Gao, J. (2019). Recent strategies on targeted delivery of thrombolytics. Asian Journal of Pharmaceutical Sciences, 14(3), 233–247. https://doi.org/10.1016/j.ajps.2018.12.004

[5] Ding, W. Y., Gupta, D., & Lip, G. Y. H. (2020). Atrial fibrillation and the prothrombotic state: revisiting Virchow's triad in 2020. Heart (British Cardiac Society), 106(19), 1463–1468. https://doi.org/10.1136/heartjnl-2020-316977

[6] Kushner, A., West, W. P., Khan Suheb, M. Z., & Pillarisetty, L. S. (2022). Virchow Triad. StatPearls Publishing.

[7] Xu, C. Q., Zeng, Y. J., & Gregersen, H. (2002). Dynamic model of the role of platelets in the blood coagulation system. Medical Engineering & Physics, 24(9), 587–593. https://doi.org/10.1016/s1350-4533(02)00047-4

[8] Qureshi, A., Lip, G. Y. H., Nordsletten, D. A., Williams, S. E., Aslanidi, O., & de Vecchi, A. (2022). Imaging and biophysical modelling of thrombogenic mechanisms in atrial fibrillation and stroke. Frontiers in Cardiovascular Medicine, 9, 1074562. https://doi.org/10.3389/fcvm.2022.1074562

[9] Chaudhry, R., Usama, S. M., & Babiker, H. M. (2023). Physiology, Coagulation Pathways. StatPearls Publishing.

[10] Brien, L. (2019). Anticoagulant medications for the prevention and treatment of thromboembolism. AACN Advanced Critical Care, 30(2), 126–138. https://doi.org/10.4037/aacnacc2019867

[11] Mackman, N. (2008). Triggers, targets and treatments for thrombosis. Nature, 451(7181), 914–918. https://doi.org/10.1038/nature06797

[12] Altiok, E., & Marx, N. (2018). Oral Anticoagulation. Deutsches Arzteblatt International, 115(46), 776. https://doi.org/10.3238/arztebl.2018.0776

[13] Steffel, J., Verhamme, P., Potpara, T. S., Albaladejo, P., Antz, M., Desteghe, L., Haeusler, K. G., Oldgren, J., Reinecke, H., Roldan-Schilling, V., Rowell, N., Sinnaeve, P., Collins, R., Camm, A. J., Heidbüchel, H., Lip, G. Y. H., Weitz, J., Fauchier, L., Lane, D., … ESC Scientific Document Group. (2018). The 2018 European Heart Rhythm Association Practical Guide on the use of non-vitamin K antagonist oral anticoagulants

in patients with atrial fibrillation. European Heart Journal, 39(16), 1330–1393. https://doi.org/10.1093/eurheartj/ehy136

[14] Wajima, T., Isbister, G. K., & Duffull, S. B. (2009). A comprehensive model for the humoral coagulation network in humans. Clinical pharmacology and therapeutics, 86(3), 290–298. https://doi.org/10.1038/clpt.2009.87

[15] Osmancik, P., Herman, D., Neuzil, P., Hala, P., Taborsky, M., Kala, P., Poloczek, M., Stasek, J., Haman, L., Branny, M., Chovancik, J., Cervinka, P., Holy, J., Kovarnik, T., Zemanek, D., Havranek, S., Vancura, V., Opatrny, J., Peichl, P., … PRAGUE-17 Trial Investigators. (2020). Left Atrial Appendage Closure versus direct oral anticoagulants in high-risk patients with Atrial Fibrillation. Journal of the American College of Cardiology, 75(25), 3122–3135. https://doi.org/10.1016/j.jacc.2020.04.067

[16] Yang, R., Zubair, M., & Moosavi, L. (2024). Prothrombin Time. StatPearls Publishing.

[17] Mendoza-Sanchez, J., Silva, F., Rangel, Lady, Jaramillo, L., Mendoza, L., Garzon, J., & Quiroga, A. (2018). Benefit, risk and cost of new oral anticoagulants and warfarin in atrial fibrillation; A multicriteria decision analysis. PloS One, 13(5), e0196361. https://doi.org/10.1371/journal.pone.0196361

[18] Kamarova, M., Baig, S., Patel, H., Monks, K., Wasay, M., Ali, A., Redgrave, J., Majid, A., & Bell, S. M. (2022). Antiplatelet use in ischemic stroke. The Annals of Pharmacotherapy, 56(10), 1159–1173. https://doi.org/10.1177/10600280211073009

[19] Zarnitsina, V. I., Pokhilko, A. V., & Ataullakhanov, F. I. (1996). A mathematical model for the spatio-temporal dynamics of intrinsic pathway of blood coagulation. I. The model description. Thrombosis Research, 84(4), 225–236. https://doi.org/10.1016/s0049-3848(96)00182-x

[20] Pearce, K. J., Nellenbach, K., Smith, R. C., Brown, A. C., & Haider, M. A. (2021). Modeling and parameter subset selection for fibrin polymerization kinetics with applications to wound healing. Bulletin of Mathematical Biology, 83(5), 47. https://doi.org/10.1007/s11538-021-00876-6

[21] Baumgartner, L., Sadowska, A., Tío, L., González Ballester, M. A., Wuertz-Kozak, K., & Noailly, J. (2021). Evidence-based network modelling to simulate Nucleus Pulposus multicellular activity in different nutritional and pro-inflammatory environments. Frontiers in Bioengineering and Biotechnology, 9. https://doi.org/10.3389/fbioe.2021.734258

[22] Burghaus, R., Coboeken, K., Gaub, T., Kuepfer, L., Sensse, A., Siegmund, H.-U., Weiss, W., Mueck, W., & Lippert, J. (2011). Evaluation of the efficacy and safety of rivaroxaban using a computer model for blood coagulation. PloS One, 6(4), e17626. https://doi.org/10.1371/journal.pone.0017626

[23] Hatoum, H., Singh-Gryzbon, S., Esmailie, F., Ruile, P., Neumann, F.-J., Blanke, P., Thourani, V. H., Yoganathan, A. P., & Dasi, L. P. (2021). Predictive model for thrombus formation after transcatheter valve replacement. Cardiovascular Engineering and Technology, 12(6), 576–588. https://doi.org/10.1007/s13239-021-00596-x

[24] Mill, J., Agudelo, V., Hion Li, C., Noailly, J., Freixa, X., Camara, O., & Dabit Arzamendi, A. (2022). Patient-specific flow simulation analysis to predict device-related thrombosis in left atrial appendage occluders. REC: Interventional Cardiology (English Edition). https://doi.org/10.24875/recice.m21000224

[25] Gasparotti, E., Fanni, B. M., Del Pia, E., Capellini, K., Danielli, F., Berti, F., Clemente, A., Berti, S., Pennnati, G., Petrini, L., & Celi, S. (2024). Computational fluid dynamic simulation to evaluate the device-related effects after left atrial appendage occlusion. En Computer Methods in Biomechanics and Biomedical Engineering II (pp. 205–212). Springer Nature Switzerland.

[26] Guerrero-Hurtado, M., Garcia-Villalba, M., Gonzalo, A., Martinez-Legazpi, P., Kahn, A. M., McVeigh, E., Bermejo, J., del Alamo, J. C., & Flores, O. (2023). Efficient multi-fidelity computation of blood coagulation under flow. PLoS Computational Biology, 19(10), e1011583. https://doi.org/10.1371/journal.pcbi.1011583

[27] Qureshi, "ahmed, Balmus, M., E. Williams, S., Y. H. Lip, G., A. Nordsletten, D., Aslanidi, O., & de Vecchi", A. (2022). Modelling virchow's triad to improve stroke risk assessment in atrial fibrillation patients. Computing in Cardiology Conference (CinC).

[28] Qureshi, A., Balmus, M., Ogbomo-Harmitt, S., Nechipurenko, D., Ataullakhanov, F., Lip, G. Y. H., Williams, S. E., Nordsletten, D., Aslanidi, O., & de Vecchi, A. (2023). Modelling blood flow and biochemical reactions underlying thrombogenesis in atrial fibrillation. En Functional Imaging and Modeling of the Heart (pp. 435–444). Springer Nature Switzerland.

[29] Méndez Rojano, R., Mendez, S., Lucor, D., Ranc, A., Giansily-Blaizot, M., Schved, J.-F., & Nicoud, F. (2019). Kinetics of the coagulation cascade including the contact activation system: sensitivity analysis and model reduction. Biomechanics and Modeling in Mechanobiology, 18(4), 1139–1153. https://doi.org/10.1007/s10237-019-01134-4

[30] Higashitani, K., Kondo, M., & Hatade, S. (1991). Effect of particle size on coagulation rate of ultrafine colloidal particles. Journal of Colloid and Interface Science, 142(1), 204–213. https://doi.org/10.1016/0021-9797(91)90047-c

[31] Williams, O., & Sergent, S. R. (2022). Histology, Platelets. StatPearls Publishing.

[32] MATLAB. (s/f). Mathworks.com. From: https://es.mathworks.com/products/matlab.html

[33] Qureshi, A. (2023). Personalised modelling of virchow's triad for stroke risk assessment in atrial fibrillation. King's collage London.

[34] Zhang, W., Li, M., Wang, X., Zhang, W., Wang, H., Li, P., & Tang, B. (2023). Precision navigation of venous thrombosis guided by viscosity-activatable near-infrared fluorescence. Analytical Chemistry, 95(4), 2382–2389. https://doi.org/10.1021/acs.analchem.2c04395

[35] Al-Azawy, M. G., Kadhim, S. K., & Hameed, A. S. (2020). Newtonian and non-Newtonian blood rheology inside a model of stenosis. CFD Letters, 12(11), 27–36. https://doi.org/10.37934/cfdl.12.11.2736

[36] Segarra-Queralt, M., Piella, G., & Noailly, J. (2023). Network-based modelling of mechano-inflammatory chondrocyte regulation in early osteoarthritis. Frontiers in bioengineering and biotechnology, 11. https://doi.org/10.3389/fbioe.2023.1006066

[37] Kwon, M.-J., Kim, H.-J., Kim, J.-W., Lee, K.-H., Sohn, K.-H., Cho, H.-J., On, Y.-K., Kim, J.-S., & Lee, S.-Y. (2009). Determination of plasma warfarin concentrations in Korean patients and its potential for clinical application. Annals of Laboratory Medicine, 29(6), 515–523. https://doi.org/10.3343/kjlm.2009.29.6.515

[38] Esmaily-Moghadam, M., Hsia, T.-Y., & Marsden, A. L. (2013). A non-discrete method for computation of residence time in fluid mechanics simulations. Physics of Fluids (Woodbury, N.Y.: 1994), 25(11), 110802. https://doi.org/10.1063/1.4819142

[39] Naito, K., & Fujikawa, K. (1991). Activation of human blood coagulation factor XI independent of factor XII. The Journal of Biological Chemistry, 266(12), 7353–7358. https://doi.org/10.1016/s0021-9258(20)89453-8

[40] Muscente, F., & De Caterina, R. (2023). The new in anticoagulation: factor XI inhibitors. European Heart Journal Supplements: Journal of the European Society of Cardiology, 25(Supplement_B), B65–B68. https://doi.org/10.1093/eurheartjsupp/suad070

[41] Camire, R. M. (2021). Blood coagulation factor X: molecular biology, inherited disease, and engineered therapeutics. Journal of Thrombosis and Thrombolysis, 52(2), 383–390. https://doi.org/10.1007/s11239-021-02456-w

[42] Franchini, M., Marano, G., Pupella, S., Vaglio, S., Masiello, F., Veropalumbo, E., Piccinini, V., Pati, I., Catalano, L., & Liumbruno, G. M. (2018). Rare congenital bleeding disorders. Annals of Translational Medicine, 6(17), 331–331. https://doi.org/10.21037/atm.2018.08.34

[43] Wolberg, A. S., & Campbell, R. A. (2008). Thrombin generation, fibrin clot formation and hemostasis. Transfusion and Apheresis Science: Official Journal of the World Apheresis Association: Official Journal of the European Society for Haemapheresis, 38(1), 15–23. https://doi.org/10.1016/j.transci.2007.12.005

[44] Duchemin, J., Pan-Petesch, B., Arnaud, B., Blouch, M.-T., & Abgrall, J.-F. (2008). Influence of coagulation factors and tissue factor concentration on the thrombin generation test in plasma. Thrombosis and Haemostasis, 99(4), 767–773. https://doi.org/10.1160/TH07-09-0581

[45] Duarte, R. C. F., Ferreira, C. N., Rios, D. R. A., Reis, H. J. dos, & Carvalho, M. das G. (2017). Thrombin generation assays for global evaluation of the hemostatic system: perspectives and limitations. Revista Brasileira de Hematologia e Hemoterapia, 39(3), 259–265. https://doi.org/10.1016/j.bjhh.2017.03.009

[46] Wolberg, A. S. (2023). Fibrinogen and fibrin: synthesis, structure, and function in health and disease. Journal of Thrombosis and Haemostasis: JTH, 21(11), 3005–3015. https://doi.org/10.1016/j.jtha.2023.08.014

[47] Ataullakhanov, F. I., Pohilko, A. V., Sinauridze, E. I., & Volkova, R. I. (1994). Calcium threshold in human plasma clotting kinetics. Thrombosis Research, 75(4), 383–394. https://doi.org/10.1016/0049-3848(94)90253-4

[48] Dintenfass, L. (1964). Viscosity and clotting of blood in venous thrombosis and coronary occlusions. Circulation Research, 14(1), 1–16. https://doi.org/10.1161/01.res.14.1.1

[49] Xia, Y., Hu, Y., & Tang, L. (2023). Factor XIa inhibitors as a novel anticoagulation target: Recent clinical research advances. Pharmaceuticals (Basel, Switzerland), 16(6), 866. https://doi.org/10.3390/ph16060866

[50] Panes, O., Matus, V., Sáez, C. G., Quiroga, T., Pereira, J., & Mezzano, D. (2007). Human platelets synthesize and express functional tissue factor. Blood, 109(12), 5242–5250. https://doi.org/10.1182/blood-2006-06-030619

[51] Hartmann, S., Biliouris, K., Lesko, L. J., Nowak-Göttl, U., & Trame, M. N. (2016). Quantitative systems pharmacology model to predict the effects of commonly used anticoagulants on the human coagulation network. CPT: Pharmacometrics & Systems Pharmacology, 5(10), 554–564. https://doi.org/10.1002/psp4.12111

[52] Rigano, J., Ng, C., Nandurkar, H., & Ho, P. (2018). Thrombin generation estimates the anticoagulation effect of direct oral anticoagulants with significant interindividual variability observed. Blood Coagulation & Fibrinolysis: An International Journal in Haemostasis and Thrombosis, 29(2), 148–154. https://doi.org/10.1097/mbc.0000000000000678

[53] Rezaeimoghaddam, M., & van de Vosse, F. N. (2022). Continuum modeling of thrombus formation and growth under different shear rates. Journal of Biomechanics, 132(110915), 110915. https://doi.org/10.1016/j.jbiomech.2021.110915

[54] Shankar, K. N., Zhang, Y., Sinno, T., & Diamond, S. L. (2022). A three-dimensional multiscale model for the prediction of thrombus growth under flow with single-platelet resolution. PLoS Computational Biology, 18(1), e1009850. https://doi.org/10.1371/journal.pcbi.1009850

SUPPORTING INFORMATION

S.1 Coagulation cascade model parameters and initial conditions

k_1	$640\ min^{-1}$	h_1	$96\ min^{-1}$	β	0.011

Table 1. Constants of the model of Xu *et al*. [1].

k_{11}	$1.1 \cdot 10^{-5}\ min^{-1}$	h_{10}	$1\ min^{-1}$	h_8	$0.31\ min^{-1}$
h_{11}	$0.2\ min^{-1}$	k_2	$2.45\ min^{-1}$	k_5	$0.17\ min^{-1}$
k_9	$20\ min^{-1}$	K_{2m}	$58\ nM$	h_5	$0.31\ min^{-1}$
h_9	$0.2\ min^{-1}$	$\overline{k_2}$	$2000\ min^{-1}$	k_{apc1}	$0.0014\ min^{-1}$
k_{10}	$0.0033\ min^{-1}$	k_{510}	$100\ min^{-1}nM^{-1}$	k_{apc2}	$0.07\ min^{-1}$
$\overline{k_{10}}$	$500\ min^{-1}$	h_{510}	$100\ min^{-1}$	k_p	$10\ nM$
k_{89}	$100\ min^{-1}nM^{-1}$	$\overline{k_{2m}}$	$210\ nM$	h_p	$1\ min^{-1}$
h_{89}	$100\ min^{-1}$	h_2	$2.3\ min^{-1}$	h_{apc}	$0.1\ min^{-1}$
k_a	$1.2\ min^{-1}nM^{-1}$	k_8	$1 \cdot 10^{-5}\ min^{-1}$	k_{3x}	$10\ min^{-1}$
k_{2x}	$7.5\ min^{-1}$				

Table 2. Constants of the model of Zarnitsina *et al*. [2] and Xu *et al*. [1].

k	1931	k_1^-	250	k_3^-	26.9
k^+	0.031	k_2^+	298	k_4^+	15.5
k^-	366	k_2^-	0.26	k_4^-	375
k_1^+	0.49	k_3^+	2.66		

Table 3. Constants of the model of Pearce *et al*. [3].

$TF{:}VIIa$	$0.005\ nM$	XIa	$0.105\ nM$	II	$867.564\ nM$	$Fbni$	$8.823 \cdot 10^6\ nM$

Table 4. Initial conditions of the model [4, 5, 6]. Tissue factor and factor VII activated complex (TF:VIIa). Factor XI activated (XIa). Prothrombin (II). Inactive fibrinogen (Fbni).

S.2 Concentrations for the sensitivity analysis

TF:VII	**XI factor**	**Prothrombin**
0.005 nM	0.105 nM	867.564 nM
0.008 nM	15.303 nM	1133.87 nM
0.01 nM	30.6 nM	1400 nM

Table 5. Concentration for each factor selected for sensitivity analysis [4, 6, 7].

S.3 P-values of the sensitivity analysis

	Thrombin peak	**Thrombin time**	**Fibrin**
TF:VII	0.86	0.73	0.82
Factor XI	7.21×10^{-16}	2.98×10^{-17}	0.38
Prothrombin	5.05×10^{-27}	1.55×10^{-29}	7.39×10^{-68}

Table 6. p-vale for each parameter and factor ($\alpha = 0.05$).

S.4 Warfarin behaviour

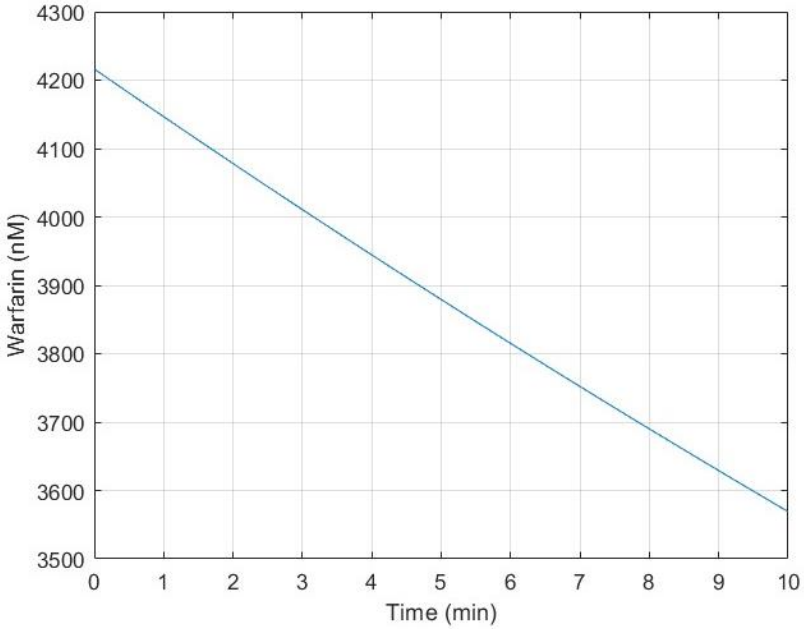

Figure 24. Concentration of warfarin as a function of time. Concentration units are in nanomolar (nM), and time units are in minutes (min).

S.5 Spatial distribution of the coagulation cascade factors in 2D

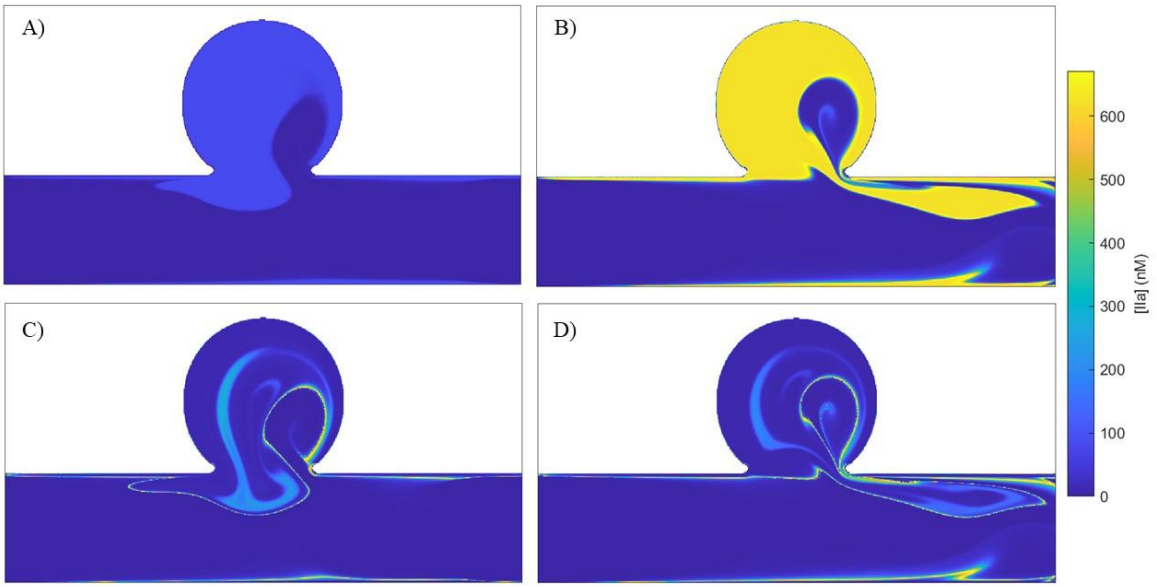

Figure 25. Thrombin (IIa) concentration distribution in the 2D geometry of an aneurysm. A) Second 24.17 of the simulation. B) Second 32.22 of the simulation. C) Second 90.23 of the simulation. D) Second 95.06 of the simulation. Concentration units are in nanomolar (nM).

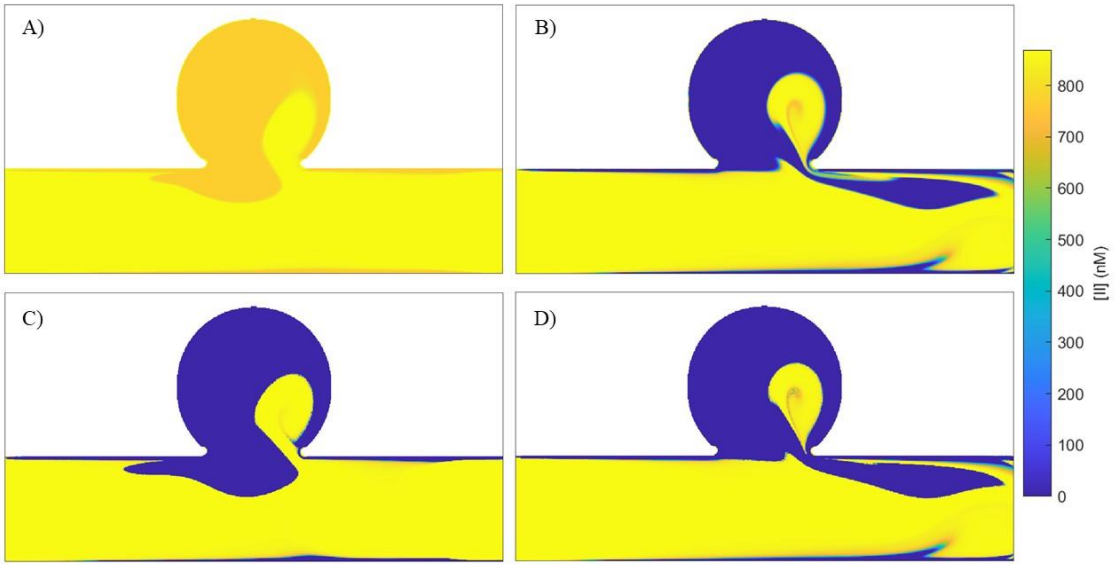

Figure 26. Prothrombin (II) concentration distribution in the 2D geometry of an aneurysm. A) Second 24.17 of the simulation. B) Second 32.22 of the simulation. C) Second 90.23 of the simulation. D) Second 95.06 of the simulation. Concentration units are in nanomolar (nM).

S.6 Spatial distribution of the coagulation cascade factors with warfarin in 2D

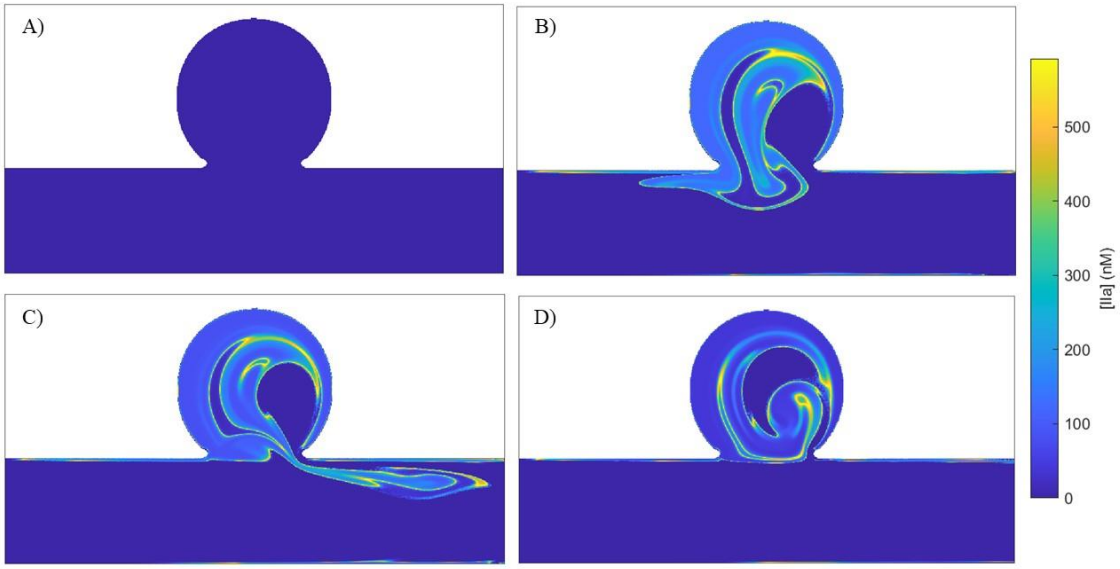

Figure 27. Thrombin (IIa) concentration distribution in the 2D geometry of an aneurysm with warfarin. A) Second 32.22 of the simulation. B) Second 90.23 of the simulation. C) Second 95.06 of the simulation. D) Second 105.53 of the simulation. Concentration units are in nanomolar (nM).

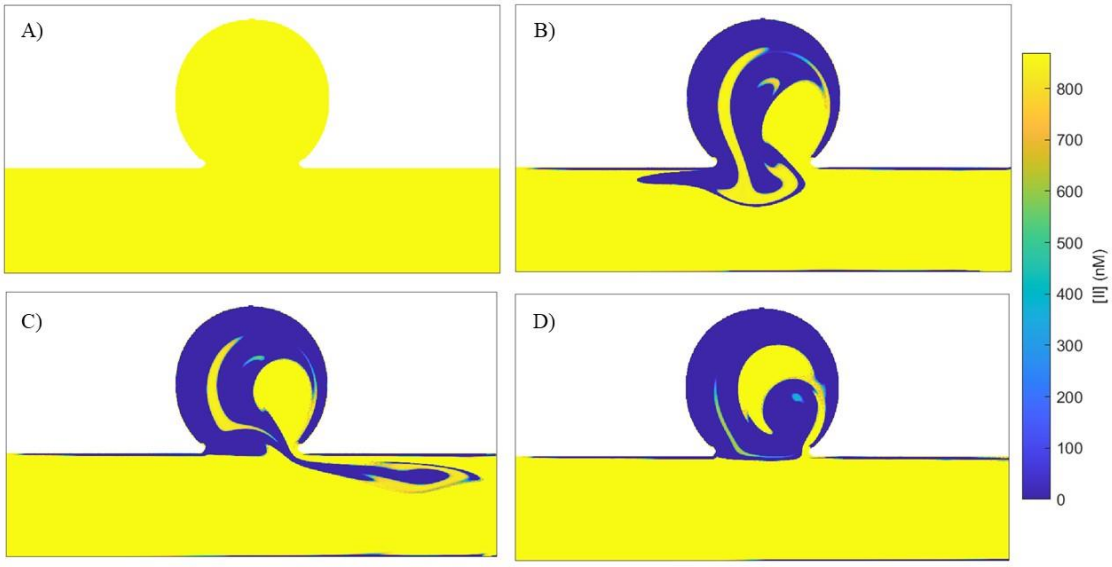

Figure 28. Prothrombin (II) concentration distribution in the 2D geometry of an aneurysm with warfarin. A) Second 32.22 of the simulation. B) Second 90.23 of the simulation. C) Second 95.06 of the simulation. D) Second 105.53 of the simulation. Concentration units are in nanomolar (nM).

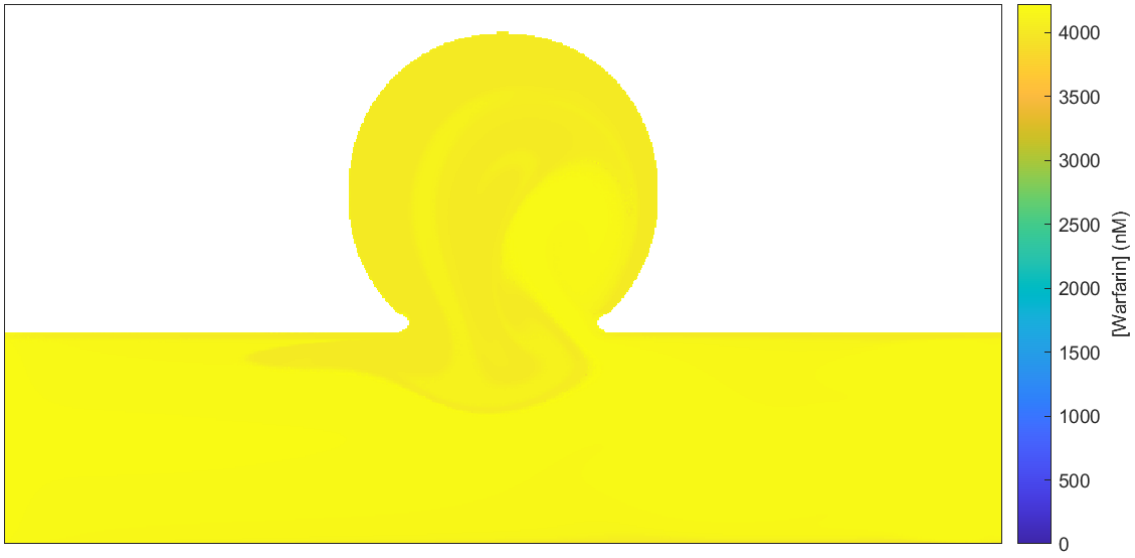

Figure 29. Warfarin concentration in second 90.23 of the simulation. Concentration units are in nanomolar (nM).

BIBLIOGRAPHY OF SUPPORTING INFORMATION

[1] Xu, C. Q., Zeng, Y. J., & Gregersen, H. (2002). Dynamic model of the role of platelets in the blood coagulation system. Medical Engineering & Physics, 24(9), 587–593. https://doi.org/10.1016/s1350-4533(02)00047-4

[2] Zarnitsina, V. I., Pokhilko, A. V., & Ataullakhanov, F. I. (1996). A mathematical model for the spatio-temporal dynamics of intrinsic pathway of blood coagulation. I. The model description. Thrombosis Research, 84(4), 225–236. https://doi.org/10.1016/s0049-3848(96)00182-x

[3] Pearce, K. J., Nellenbach, K., Smith, R. C., Brown, A. C., & Haider, M. A. (2021). Modeling and parameter subset selection for fibrin polymerization kinetics with applications to wound healing. Bulletin of Mathematical Biology, 83(5), 47. https://doi.org/10.1007/s11538-021-00876-6

[4] Guerrero-Hurtado, M., Garcia-Villalba, M., Gonzalo, A., Martinez-Legazpi, P., Kahn, A. M., McVeigh, E., Bermejo, J., del Alamo, J. C., & Flores, O. (2023). Efficient multi-fidelity computation of blood coagulation under flow. PLoS Computational Biology, 19(10), e1011583. https://doi.org/10.1371/journal.pcbi.1011583

[5] Butenas, S., Orfeo, T., & Mann, K. G. (2009). Tissue factor in coagulation: Which? Where? When? Arteriosclerosis, Thrombosis, and Vascular Biology, 29(12), 1989–1996. https://doi.org/10.1161/atvbaha.108.177402

[6] Winter, W. E., Greene, D. N., Beal, S. G., Isom, J. A., Manning, H., Wilkerson, G., & Harris, N. (2020). Clotting factors: Clinical biochemistry and their roles as plasma enzymes. En Advances in Clinical Chemistry (Vol. 94, pp. 31–84). Elsevier.

[7] Wajima, T., Isbister, G. K., & Duffull, S. B. (2009). A comprehensive model for the humoral coagulation network in humans. Clinical pharmacology and therapeutics, 86(3), 290–298. https://doi.org/10.1038/clpt.2009.87